Sensing and Bio-Sensing Research 43 (2024) 100606

Contents lists available at ScienceDirect

Sensing and Bio-Sensing Research

journal homepage: www.elsevier.com/locate/sbsr

Thermo-cyclically operated metal oxide gas sensor arrays for analysis of dissolved volatile organic compounds in fermentation processes: Part II – Quasi online monitoring in biogas fermentation

Binayak Ojha [a,*], Andreas Wilke [b], Regina Brämer [b], Matthias Franzreb [c], Heinz Kohler [a,*]

[a] Institute for Sensor and Information Systems (ISIS), Karlsruhe University of Applied Sciences, Moltkestr. 30, D-76133 Karlsruhe, Germany
[b] Offenburg University of Applied Sciences, Badstr. 24, D-77652 Offenburg, Germany
[c] Institute of Functional Interfaces (IFG), Karlsruhe Institute of Technology (KIT), Hermann-von-Helmholtz-Platz 1, D-76344 Eggenstein-Leopoldshafen, Germany

ARTICLE INFO

Keywords:
Metal oxide
Gas sensor array
Thermo-cyclic operation
Volatile fatty acid monitoring
Biogas fermentation

ABSTRACT

This study presents a quasi-online method for monitoring of dissolved volatile fatty acids (VFAs) in biogas fermentation processes with a carrier gas probe by use of thermo-cyclically operated metal oxide gas sensor arrays. Each of the two sensor arrays comprises a pure SnO_2 and three different SnO_2/additive-composites (additives: alumina, YSZ, NASICON) but differ by SnO_2 synthesis routes, namely Flame Spray Pyrolysis (FSP) and Sol-Gel (SG) technique, respectively. This allowed comparative studies of the influence of layer morphology on VFA sensing characteristics. For sensitive determination of the dissolved VFAs besides high concentrations of biogas components like CO or CH_4, first a pre-treatment routine of the fermentation sample was introduced to remove those physically dissolved gases without losing VFAs. The Conductance-over-Time-Profiles (CTPs) of eight different sensing layers were measured simultaneously at exposure to the gases extracted from the fermentation sample at different pH conditions. Almost all the investigated SnO_2/additive-composites show CTP-features clearly correlating with the undissociated VFA even at concentrations below 120 ppm as referenced by GC-analysis. The lower detection limit is well below inhibitory concentration for fermentation processes. As expected, most pronounced CTPs representing actual VFAs situation were measured at pH 3, well below the pKa of the VFAs. The FSP-layers highlighted clearly better sensitivity and CTP specificity of higher quality compared to SG-layers. Among the SnO_2/additives, the CTP-features of the SnO_2(FSP)/NASICON and SnO_2(SG)/NASICON layers showed the best specificity to acetic and propionic acid. For the first time, quasi-online analysis of VFAs using metal oxide gas sensors for early warning of VFA-development in biogas fermentation processes was demonstrated.

1. Introduction

With increasing demand for non-fossil and green energy, interest in biogas production by anerobic digestion of organic materials from domestic and industrial organic wastes is rapidly increasing. This well established biotechnological method has promised to enable utilizing wide range of organic wastes, such as livestock waste [1–4], municipal solid waste [1], agricultural waste [3,5,6], food waste [4], etc., for anaerobic co-digestion to produce green energy, which in future may lead to an extensive organic waste management.

However, anerobic digestion is a complex biochemical process which involves several steps of metabolic gasification reactions like hydrolysis, acidogenesis, acetogenesis and methanogenesis [7]. The resulting biogas is mainly composed of methane and carbon dioxide, with traces of intermediate products like hydrogen, carbon monoxide, hydrogen sulfide and volatile organic compounds (VOCs) such as, alcohols, and volatile fatty acids (VFAs), in particular acetic acid, propionic acid and butyric acid.

The continuous monitoring and control of the biogas fermentation processes for biogas production is desirable because it allows to run the fermentation process at maximum rate and enables long-term process stability. There are several commonly used physical and biochemical indicators like pH, alkalinity ratio [8], FOS/TAC (volatile organic acids/total inorganic carbonate) [9], gas production rate, and gas composition [10–12], which give crude information with regard to the system stability. Additionally, even the developments of hydrogen [13,14] and

* Corresponding authors.
E-mail addresses: binayak.ojha@h-ka.de (B. Ojha), heinz.kohler@h-ka.de (H. Kohler).

https://doi.org/10.1016/j.sbsr.2023.100606
Received 17 September 2023; Received in revised form 4 November 2023; Accepted 13 November 2023
Available online 14 November 2023

carbon monoxide [14] are considered as process indicators. However, most of these indicators can only represent very gradual changes in the process.

It is well acknowledged that the key sensitive indicators, representing the process status used for early warning of a possible breakdown, are some undesired intermediate products like the VFAs [11,15–19]. In a stable fermentation process, VFAs are formed as intermediate products in acidogenesis phase, but are converted to acetate consuming hydrogen in the acetogenesis phase and are ultimately decomposed to methane and carbon dioxide in methanogenesis phase [20]. Acidification of the fermentation substrate is one of the key reasons for process breakdown in anerobic digestion [21]. In particular, high acetate concentrations inhibit the acetogenesis process as well as the propionate degradation (in acidogenesis phase) resulting in the accumulation of organic acids [7]. Thus, acetic acid and propionic acid [22,23] concentrations are crucial parameters to be monitored. In addition, the propionate to acetate ratio is also considered as an important process indicator [7,24]. The concentration of these two VFA-components beyond a certain threshold level can cause system instability. Therefore, continuous monitoring of these individual VFAs is assumed to provide quick and important information about the actual status of the anerobic digestion process [25]. Knowledge of these indicators allows to take preventative action to optimize the fermentation process continuously e.g. by adaptation of the feed, and, in critical cases, early warning of upcoming breakdowns [10,26]. However, the threshold concentration level for the individual VFAs is not well defined, but is generally rather low. It varies for different fermentation processes and depends on the composition of the substrate and other operating conditions [12].

In this respect, it is very much desired to have a sensor system for detecting the real time change of the individual VFA concentrations prior to complete process failure and to use this analytical information with feedback control systems for an advanced automated process control to avoid such VFA-developments and to optimize the biogas fermentation process [17].

The other way round, biotechnological cultivation of VFAs does also drive interesting applications. In recent years, different studies have shown that VFAs produced during anaerobic digestion of organic wastes are promising substrates for several second-step refinements, such as sustainable biofuels like biodiesel [27,28] and biopolymers like Polyhydroxyalkanoates [29]. In this context, in contrast to the biogas fermentation process, the anaerobic digestion process is tweaked to produce VFAs as the major product and a sensor system for monitoring of the production of the VFAs is indeed desirable.

The well-established and commonly used offline methods for the analysis of the VFAs are titration methods [19,30], gas chromatography (GC) [31] or high-performance liquid chromatography (HPLC) [16]. Analysis by titration is the most simple method which provides the total VFA concentration at relatively low costs but fails to identify the concentration of the individual VFA components. In addition, there are some methods reported about the online analysis of VFA in biogas fermentation processes by introduction of in-situ filtration techniques of the fermentation sample using a rotating pre-filter with an ultra-membrane in combination with a GC [15]. However, the major concerns with the membrane and filters are frequent fouling issues requiring a high level of maintenance. This limitation is overcome by extraction of the gas from the headspace of the reactor for GC analysis [10]. GC and HPLC methods are considered highly accurate and reliable, but require high service efforts to avoid any contamination of column which may lead to drift in the baseline avoiding accurate analysis, which makes them economically unfeasible. Similarly, several other online methods for VFA monitoring in biogas fermentation processes using light sources, such as UV spectroscopy [32–34], Near IR spectroscopy [35,36], Mid IR spectroscopy [16], and Spectrofluorimetric spectroscopy [20] are reported. These analysis methods are without doubt interesting, however, again all these methods have in common that they are limited by their high service efforts, e.g. to keep deposition of molecules on the windows of the excitation chamber at an acceptable level.

Quite recently, some innovative biosensors, such as a bio-electrolytic sensor [37] and hybrid biosensor arrays [38] were reported for the online measurement of VFAs in biogas fermentation processes. The former one is based on a microbial electrolysis cell. The sensor signal represents the total VFA concentration, which could be linearly correlated with VFA concentrations in the range 0–7000 ppm. However, it does not allow the analysis of the individual VFAs. Stable and maintenance free operation of those sensors in lab over 5 months is reported. However, for applications in the fullscale reactors, an online sampling and sensing system is reported to be still missing. The biosensor array [38] works according to the amperometric principle. It integrates several analyte-sensing Pt-electrodes loaded with different enzymes selective for different analytes such as acetate, propionate, formate, ethanol, L-lactate and D-lactate. But a common procedure for sample preparation, which would be suitable for different sensing electrodes and different analytes like VFAs (acetate and propionate) and other targets such as formate, ethanol-lactate and D-lactate is not yet available. Nevertheless, the biosensor system is reported to be applied for long-term monitoring of a lab-scale biogas reactor (0.01 m^3) for a period of 2 months and successfully monitored 0–2500 ppm of acetic acid and 0–1500 ppm of propionic acid. However, the information about the maximum concentration limit of measurement is not available.

Another well-established method for analysis of dissolved VOCs was already introduced in [39,40]. Dissolved VOCs are extracted from the aqueous liquid phase via a carrier gas probe covered by a gas permeable membrane. This method was proven to be quite robust and provides the advantage that all ionic components per se cannot percolate the gas permeable membrane and, therefore, do not contribute to cross-sensitivity. In good approximation the VOC concentration in the carrier gas (synthetic air) depends linearly on the VOC concentration in the liquid in case of constant carrier gas flow. The carrier gas loaded with the analyte is transported to a gas sensor cell outside the fermentation reactor for analysis. In general, excellent candidates for VOC detection are metal oxide gas sensors (MOGs). However, this type of sensor suffers on cross-sensitivities to a big number of oxidizable gas components, as for instance CH_4, CO, H_2, etc., which are all components of biogas. So, special procedures for sample conditioning are necessary to enable monitoring of low concentrations of VFA developing in the fermentation process in presence of high concentrations of biogas. For this purpose specific metal oxides had to be found in a screening of SnO_2/additives, which are highly sensitive to the VFAs [40]. The authors reported about different thermo-cyclically operated sensor arrays consisting of different SnO_2/additive gas sensing layers fabricated in two different kinds of morphology. Some show excellent sensitivity and gas specific Conductance-over-Time-Profile (CTP) features characterizing the composition of dissolved VFAs like acetic acid and propionic acid even at low concentrations (about 100 ppm). This makes them promising candidates for VFA monitoring in biogas fermentation.

In this work, the authors present preliminary studies of those sensor arrays when utilized for quasi online in-situ analysis of dissolved VFA in the biogas fermentation process. CTPs recorded by exposure of analyte gas extracted from the liquid fermentation sample by the use of a gas carrier probe at constant carrier gas flow are compared with previously recorded CTPs measured for different model VFAs dissolved in DI water [40]. The detailed experimental procedure is described in Sec. 3.1. From earlier investigations it can be expected that if those CTPs of the fermentation sample are gas specific enough and comparable with the model VFAs, numerical analysis allows even discrimination between different VFA components [39,41,42]. For the experimental validation of this concept of in-situ analysis of dissolved VOC even for the monitoring of the development of VFA in fermentation processes, a fermentation matrix was prepared in the laboratory and the CTPs of different SnO_2/additive layers were recorded at different pH conditions. The VFA concentration states as developed in the fermentation process and further simulated by manual addition of well-defined volumes of the

acetic and propionic acid were referenced by gas chromatography (GC) and correlated with the corresponding changes of the CTPs. All these aspects, namely the method of fermentation matrix conditioning, the change of the CTPs with fermentation matrix conditioning, and how CTPs change with VFA-concentration, are presented and discussed in the following sections. Some preliminary results comparing CTPs recorded with model VFAs with those with fermentation sample are reported and the challenges of in-situ analysis of dissolved VFA in biogas fermentation process using the above-mentioned method are discussed.

2. Materials and methods

2.1. Fermentation matrix

The fermentation matrix was prepared with a biological substrate from a sewage plant in two glass reactors (1 l volume each) with a stainless-steel top cover providing outlet for biogas collection. Over several months at room temperature condition, it was fed with beer marc dried at 60 °C for several days and wood juice [43,44]. The latter material was mechanically dewatered from wood chips using a wood chip squeezer. 50 ml of wood juice and 10 mg of beer marc were fed in intervals of 3 to 4 days. The pH of the sample was frequently monitored and was typically in the range of 6.5–6.8. For sensitivity test measurements (Sec. 3.1) 500 ml of the fermentation matrix from each glass reactor was transferred to the analysis-reactor (1 l volume) and well admixed by continuous stirring.

2.2. MOG sensor arrays

The identical two MOG sensor arrays (chip size: 4 × 4 mm^2) as described in [40], each comprising four different metal oxide (MO) layers deposited on Pt- IDEs with a Pt-temperature sensor at the top side and a Pt-heater at the reverse side, are used for the analysis experiments of the dissolved VFAs in the fermentation matrix. Each sensor array provides four different sensitive layers, namely pure SnO_2, SnO_2/Alumina, SnO_2/YSZ and SnO_2/NASICON, however, the SnO_2-powder of one array was prepared on a sol-gel route (SG) and that of the other array was prepared by a flame spray pyrolysis technique (FSP). Correspondingly, for distinction, the layers are labeled as SnO_2(SG)/additive and SnO_2(FSP)/additive. Beyond the typical limits of preparation reproducibility by the micro dispensing technique, both kinds of MO-layers differ characteristically in morphology/porosity and layer thickness. The preparation details of each kind of sensitive layers and their comparison with respect to thickness, morphology and particularly gas response characteristics as investigated, are described in detail in part I [40].

The sensor arrays were operated in a sensor measurement cell in a thermo-cyclic mode at temperatures between 150(±5) °C and 450(±5) °C using a triangular heating voltage with a cycle period of 15 min (Fig. 1a). The actual surface temperature of the sensor array chip was estimated from the actual resistance of the Pt-resisitive temperature sensor [40] after calibration in a temperature controlled tubular furnace in advance. The sensor measurement cell provides holders for two sensor array chips, which were exposed to analyte gases simultaneously. Generally, the CTPs of all the sensitive layers on both sensor arrays were measured simultaneously together with the temperature sensor resistance at 128 sampling points of a cycle period. From the measured CTPs, absolute sensor response (R) is calculated as the integral of the CTPs according to Eq. (1). G_x is the conductance at a sampling point x and n is the total number of the samping points in one measurement cylce; in this case $n = 128$.

$$R = \sum_{x=0}^{n} G_x \tag{1}$$

Prior to the measurements with the fermentation matrix, the sensing properties of all the sensitive layers of both sensor arrays towards different concentrations of acetic acid, propionic acid, ethanol and acetone dissolved in DI water were investigated [40]. Each sensitive layer showed characteristic CTP-shapes representing the individual surface reaction processes with individual analyte and could be identified as good candidates for monitoring of the VFAs in the biogas fermentation process. Here, as an example, CTP profiles of SnO_2(FSP)/NASICON when exposed to different VOCs like acetic acid, propionic acid, ethanol and acetone dissolved in DI water are shown in Fig. 1b and Fig. 1c.

2.3. Measurement concept for in-situ analysis of VFAs dissolved in fermentation matrix

The concept of in-situ analysis of VOCs dissolved in DI water by operation of a carrier gas probe (CGP) complemented with a thermo-cyclically operated MOG sensor array, was already introduced in [40]. However, for in-situ analysis of dissolved VFAs in anaerobic digestion requires a special pre-conditioning treatment of the fermentation matrix due to the well-known cross-sensitivity of MOG sensors to biogas components (CH_4, CO, H_2, etc.) and other intermediate VOCs developing at

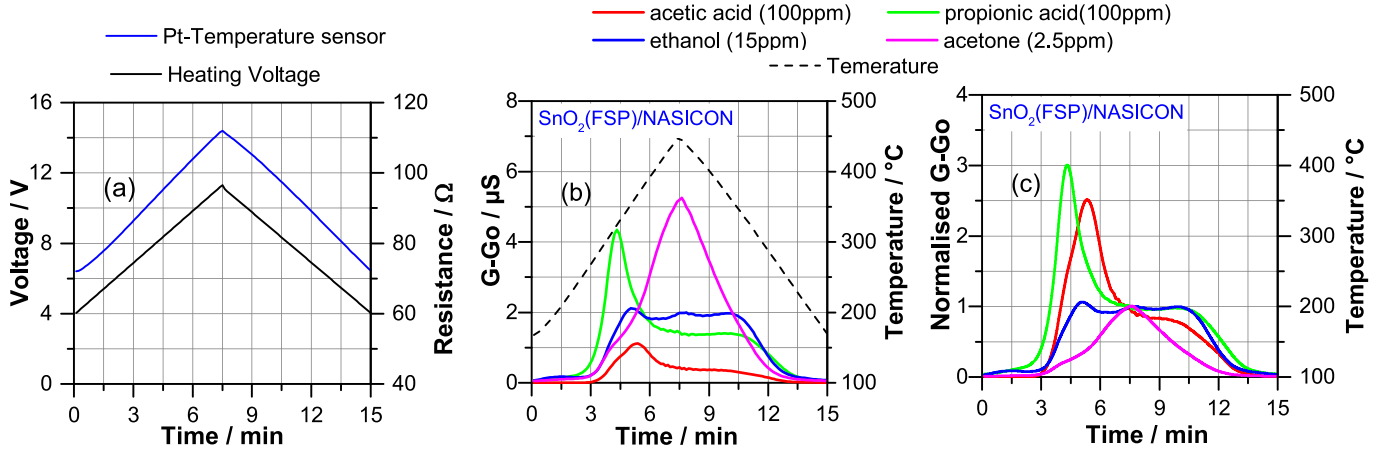

Fig. 1. Sensor response of the SnO_2(FSP)/NASICON-layer at thermo-cyclic operation. (a) Heater voltage over one temperature cycle (black) and corresponding temperature sensor resistance (blue). (b) Temperature profile (dotted line) of a heating cycle and CTPs (G-Go) at exposure to different VOCs (acetic acid, propionic acid, ethanol, and acetone) dissolved in DI water at pH 3 condition. Go is Go(hum. air) i.e., the CTP measured in DI water at pH 7. G is the CTP response measured in presence of the VOC-analyte dissolved in DI water at pH 3 (c) Normalized CTPs related to the conductance value measured at maximum temperature (b). (For interpretation of the references to colour in this figure legend, the reader is referred to the web version of this article.)

these process conditions. The pre-conditioning treatment is described below in a more general manner:

In a first step, a well-defined volume of the biogas fermentation matrix is extracted from the main reactor and transferred to another reactor (here, this is the reactor used for the experiments), which could be referred as the analysis-reactor. The required volume of the extracted sample depends on the volume of the analysis-reactor with a criterion that the silicon rubber membrane of the CGP in the analysis-reactor is completely immersed in the fermentation sample (necessary for proper analysis with CGP). For transformation of the dissolved organic acids to the dissociated state, pH of the sample is first shifted to an alkaline value (pH 8) by dosage of potassium hydroxide. Now, purging out of the biogas and all other non-dissociated and physically dissolved gas components which may contribute to the sensor signal is possible by a high flow of inert gas like N_2 without loss of dissolved VFAs.

After this purging procedure, a first CTP, called as (CTP-ref), is sampled for reference at the same operation conditions of the CGP as used for the later measurements. This CTP-ref may represent all residual gas components (water vapor, residual biogas, etc.) at this pH-condition, but per se is formed without the VFAs, because their pKa is at about pH = 4.8 (Fig. 2), i.e., well below the actual pH condition (pH = 8). Using CGP enables the uptake of undissociated molecular dissolved organic acids from the liquid state into the constant flow of synthetic air (carrier gas: 5 ml/min) by permeation through the gas permeable silicon rubber membrane. Via the carrier gas, the permeated gas molecules are transported to the MOG sensor arrays for analysis at condition of high and constant oxygen concentration determined by the kind of carrier gas (synthetic air). The latter aspect is important for reliable gas analysis with MOG sensors in general.

In the second step, the pH is now shifted (in steps) to pH 3 which is clearly lower than the pKa value of the organic acid dissociation equilibria under investigation. This is achieved by dosage of phosphoric acid. Now, the organic acids are dissolved in molecular state (Fig. 2) and, correspondingly, the partial pressure of these molecules is now high depending on their liquid phase concentration according to Henry's law. This induces diffusion across the gas permeable membrane and is reflected in a gas component specific change of the CTP features in relation to the CTP-ref sampled at pH 8 condition. As already demonstrated in [40], there was a good but individual correlation between the concentration of the organic acid compound in the liquid phase and the integral of the CTPs observed in the concentration range under investigation following a power law [40].

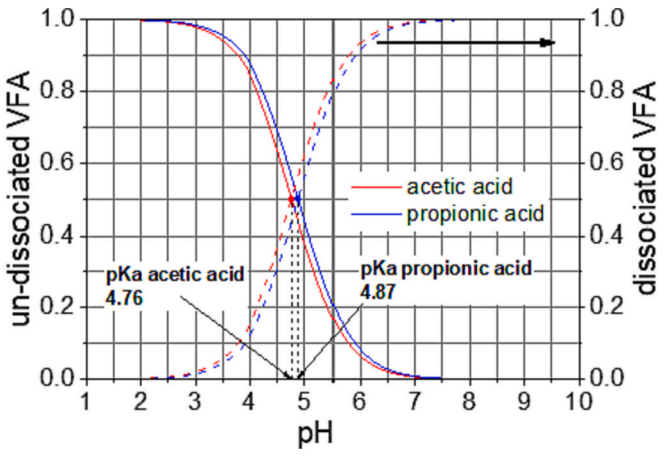

Fig. 2. Equilibria curves of relative dissociated and undissociated state concentrations of acetic and propionic acid vs. pH-value.

3. Experimental

3.1. Test setup and measurement sequence for evaluation of the VFA analysis concept

The experimental setup used for the analysis of VFAs dissolved in a real biogas fermentation matrix is illustrated in Fig. 3. In a thermostated (18 °C) glass fermentation reactor (analysis-reactor) the homogeneity of the sample is maintained by continuous stirring. Optimized constant carrier gas flow (5 ml/min synthetic air) in CGP [40] was set by a commercial mass flow controller (MFC1) when the 3-way magnetic valve was set in position (2) (Fig. 3a). The gaseous analyte extracted from the fermentation matrix was led to the measurement cell consisting of two thermo-cyclically operated MOG sensor arrays (Fig. 3, Sec. 2.2). Alternatively, as per requirement the sensor arrays have to be exposed by synthetic air, the 3-way magnetic valve is set to position (1). This is typically necessary during refilling of the reactor with new bio fermentation sample for analysis and during purging of the fermentation sample by a continuous flow of N_2 (500 ml/min) as adjusted with MFC2 (Sec. 2.3, first step procedure, Fig. 3b). At this procedure, the 3-way hand valve has to be adjusted to enable "gas out".

A Keysight 34970A data acquisition unit operates the MFCs, the 3-way magnetic valve and measures the 128 conductance sampling points per temperature cycle of each gas sensitive layer and the resistive temperature sensor of both sensor arrays, simultaneously. The corresponding triangular heating voltages for continuous temperature cycling of the sensor array chips are generated by the D/A- converters of the same data acquisition unit.

The measurement sequence over time is given in Fig. 4. The whole experimental sequence can be divided into three different phases. The first phase (Fig. 4a) is sample pre-conditioning (0–1.75 h) in which 1 l of the fermentation matrix, now called analysis sample (Sec. 2.1), is transferred to the analysis-reactor. The initial pH of the sample (about 6.7) is shifted to an alkaline value (pH 8) by dosage of potassium hydroxide (5.34 M KOH) at 1 h and, subsequently, all gaseous components dissolved are purged out by a N_2-flow (500 ml/min) for 45 min. During this sample pre-conditioning phase, the sensor arrays were exposed to dry synthetic air (flow 5 ml/min).

In the second phase (1.75-25 h, Fig. 4b), gaseous analyte is continuously extracted from the analysis sample via CGP (carrier gas flow 5 ml/min, 3-way magnetic valve (Fig. 3) at setting 2) and led to the sensor arrays for analysis. As illustrated in Fig. 4b, the sensor signals were recorded chronologically at different pH values (pH 8 → pH 5 → pH 3.85 → pH 3). Decrease of the pH in steps was achieved by dosage of phosphoric acid (8.67 M H_3PO_4). Similarly, in the third phase (25-34 h, Fig. 4c), sensor signals were recorded at pH 3 condition after manual dosage of different volumes of acetic and propionic acids, which correspond to concentrations as indicated, all related to the original state of fermentation matrix at pH 3 condition.

3.2. Methods of gas analysis referencing

For correlation of the CTP-signals as recorded from the two sensor arrays when exosed to different gas conditions in general and the CTP-changes measured with change of pH of the analyte in particular, reliable classical gas analysis methods were necessary for referencing purposes. Simultaneous FTIR analysis of the analyte was preferred for this purpose by use of a flow through setup (Sec. 3.2.1) because it allows continuous gas analysis simultaneous to the CTPs of the different sensitive layers recorded. In addition to FTIR-analysis, batch-wise analysis of individual samples extracted at every pH–state was made by GC analysis.

3.2.1. FTIR-analysis

For analysis of the analyte extracted via the CGP, a TENSOR II FTIR Spectrometer (Brucker Optik GmbH, Germany) was operated

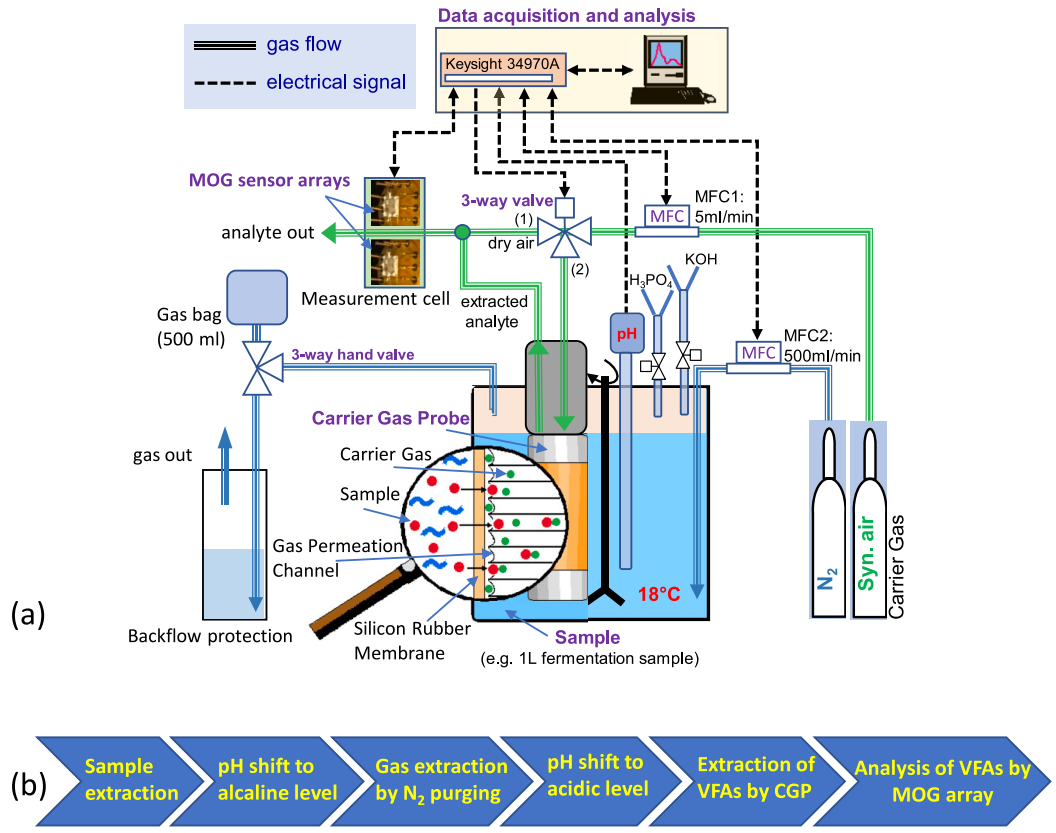

Fig. 3. Concept for analysis of VFA dissolved in biogas fermentation liquid. (a) Experimental setup, (b) scheme of the sequence of operation.

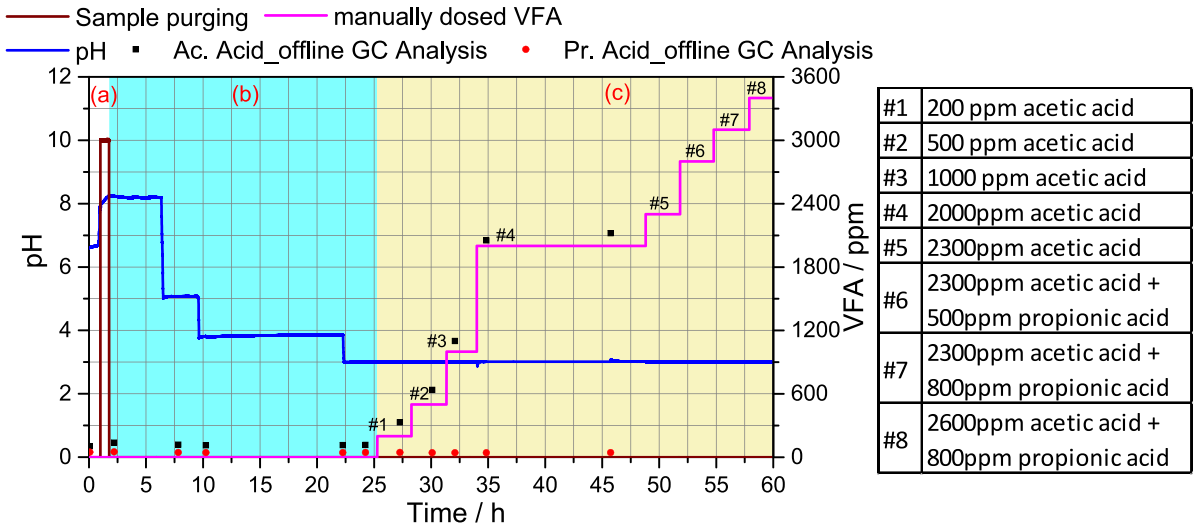

Fig. 4. Sequence of sample treatment for CTP-measurements over time referenced by GC analysis. (a) Sample pre-conditioning, (b) course of pH-change in steps. (c) Steps of acetic/propionic acid dosage over time at pH 3. The concentrations indicated relate to the manually dosed volumes.

simultaneously to CTPs measurements (Sec. 3.1). To optimize sensitivity of the FTIR-spectra, a special optical flow-through measurement cell with length and open diameter optimized with respect to the optical conditions of the instrument was constructed and installed in the setup as visualized in Fig. 5a. This measurement cell, complemented by two KBr windows on either side, ensured the analyte flow-through measurement by a maximum optical path-length given by the spacing of the measurement chamber and helped to adapt the cell-volume to the low flow rate (5 ml/min) of the analyte extracted by CGP.

With this setup, two FTIR gas analysis procedures were investigated. (i) For simultaneous CTP sampling and FTIR-analysis, the analyte gas from the carrier gas probe was first lead into the sensor cell and then to the optical flow-through cell of the FTIR (Fig. 5b). This method provides direct, i.e. simultaneous correlation of the CTPs recorded with the FTIR-spectra. However, the sensitivity achieved suffers on non-negligible gas consumption by the two MOG sensor-chips.

In order to achieve some further correlations of the CTP-changes observed with respect to the composition of the gas released especially at pH-transition from 8 to 5 (Sec. 4.1), separate experiments were conducted with the remaining fermentation matrix (1 l) (Sec. 2.1) by

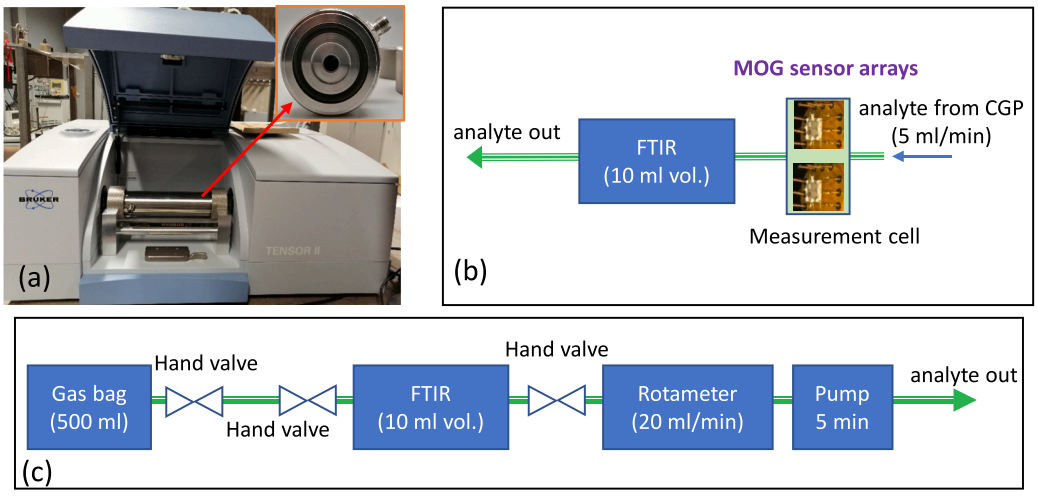

Fig. 5. (a)Tensor II FTIR Spectrometer with modified measurement cell (length: 200 mm, diameter: 10 mm and volume: 10 ml). (b) Schematic showing the arrangement for online FTIR analysis. (c) Arrangement of offline FTIR analysis of the gaseous sample collected in gas bag.

repetition of the same experimental protocol for sample treatment (Fig. 4). However, these experiments were done without GC analysis and without exposure of the MOG sensor arrays to these gases released by the fermentation process. In this experiment, clearly better analysis results with respect to the sensitivity of the FTIR-absorption bands were achieved by (ii) collection of the analyte gas from the headspace

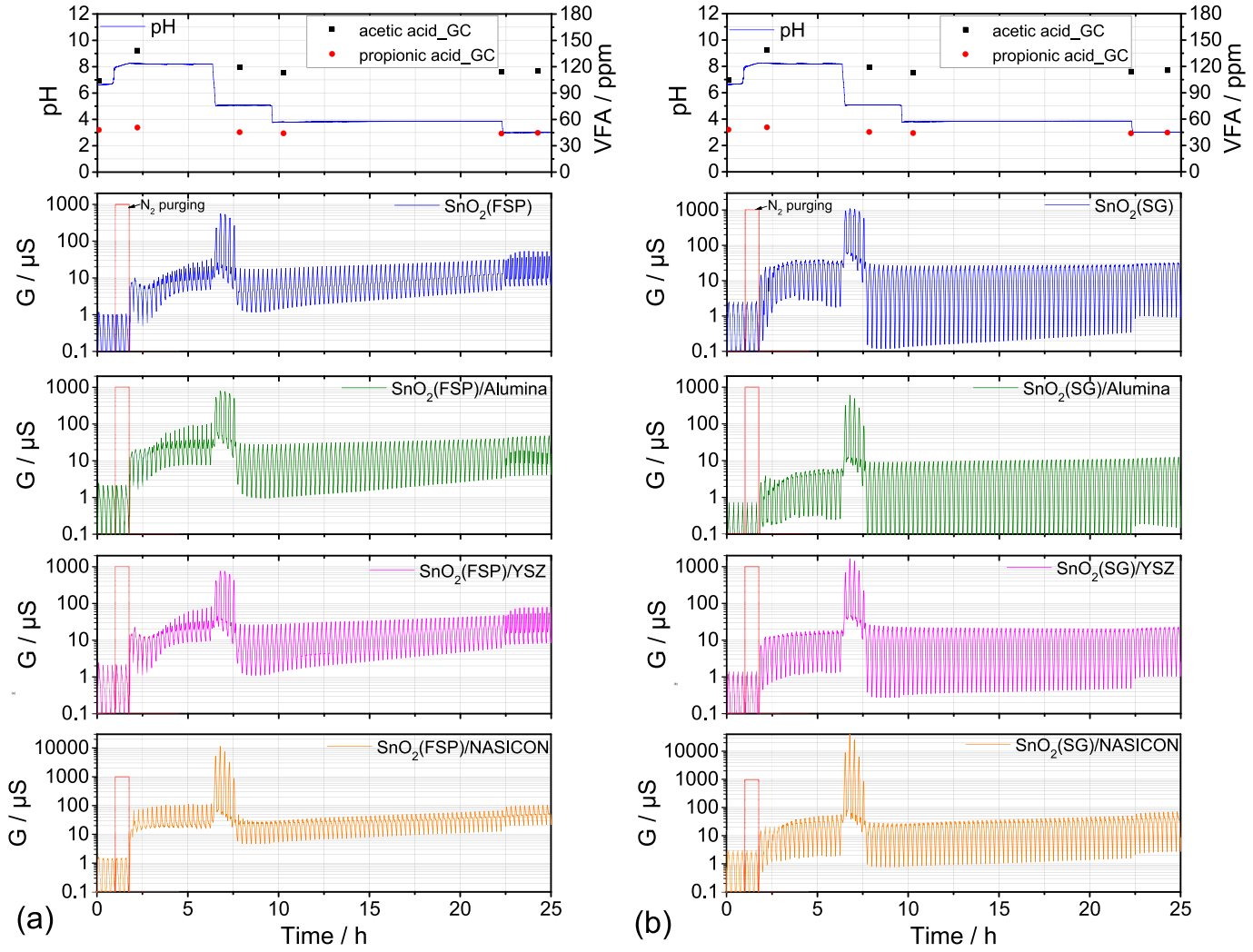

Fig. 6. GC analysis results and sensor response (CTP) of different SnO_2/additive-layers vs. time at different pH conditions of the fermentation matrix. (a) SnO_2(FSP)/additive-layers and (b) SnO_2(SG)/additive-layers. Sample pre-conditioning phase: 0–1.75 h.

(Fig. 3a) in a gas bag with the help of a 3-way hand valve (Fig. 3a) and offline FTIR analysis afterwards (Fig. 5c). The gas collected in the gas bag was guided to the FTIR measurement cell (volume: 10 ml, Fig. 5a) at constant flow rate of 20 ml/min with the help of a pump and a rotameter. After complete purging of the residual gas component in the measurement cell over 5 min, the hand valves at either side of the measurement cell (Fig. 5c) were simultaneously closed for subsequent FTIR offline analysis.

3.2.2. GC-analysis

For additional offline analytical referencing at situations as indicated in Fig. 4, 20 ml of the fermentation matrix were extracted, centrifuged at 3000 rpm for 5 min and then stored in a freezer. The concentration of acetic acid, propionic acid, byutric acid and isobyutric acid of these samples was analyzed using a gas chromatograph (GC-456 Scion Instruments). Prior to the gas chromatography (GC) analysis, the samples were centrifuged at 10400 rpm at 8 °C to get particle free analytes.

4. Results and discussion

In this Sec., the CTPs of the eight MO-layers measured simultaneously at different fermentation sample conditions (pH-value) are visualized and their validity with respect to VFA analysis capability is discussed.

4.1. Sensor response (CTPs) at different pH condition of the fermentation sample

The response of SnO_2(FSP)/additive-layers (Fig. 6a) and SnO_2(SG)/additive-layers (Fig. 6b) was measured over time according to the procedure as introduced in Fig. 4b and is illustrated for different pH conditions in Fig. 6. The corresponding CTPs of eight different MO-layers provided on two sensor arrays (Fig. 3) are visualized in Fig. 8. Furthermore, Table 1 shows the GC analysis results sampled at different times of the sequence of sample treatment (Figs. 4 and 6).

In the sample pre-conditioning phase (0–1.75 h, Fig. 6), the sensor arrays were continuously exposed to dry synthetic air and purging treatment of fermentation sample with N_2 (1–1.75 h, Fig. 6) was introduced to remove the un-dissociatively and physically dissolved biogas components like CH_4, H_2, CO, etc. from the analysis sample, which are expected to produce cross sensitivity at the MO-layers with respect to the VFA measurements. Immediately after N_2-purging, the sensor arrays were exposed to the gas extracted from the analysis sample at pH 8 via the CGP. This moment is indicated by the rise of sensor responses at 1.75 h (Fig. 6). At this pH-condition, the VFAs are expected to be completely in dissociated state (Fig. 2) and the recorded sensor signals do not represent any VFAs but mainly represent the response to humidified air and, perhaps, some residual physically dissolved biogas components (CO, H_2, CH_4, etc.) and very low concentrations of other residual non-dissociated VOCs in the fermentation sample. Thus, the CTPs measured at this sample condition, e.g., the CTPs pH 8@3 h (Fig. 8), are observed clearly higher than the CTPs measured at dry synthetic air exposure but are considered as the baseline of the VFA analysis. They do not represent the small but significant acetate and propionate concentration present in the analysis sample as indicated by GC analysis (Table 1, Fig. 6).

Table 1
Acetic and propionic acid concentrations as estimated by the GC analysis probed at different times of the measurement sequence (Figs. 4 and 6).

Time / h	acetic acid / ppm	propionic acid / ppm
0.2	104	48
2	138	51
8	119	45
10	113	44
22	114	44
24	115	44
27	330	44
30	636	42
32	1100	42
35	2051	43
46	2120	44

Furthermore, very most MO-layers show a clear increase of the absolute sensor signal (Fig. 6) with time in time-interval 1.75–6.5 h. This is illustrated even better by the enhancement of specific features of the corresponding CTPs (Fig. 8) of all MO-layers at around 1.5–3 min (compare CTPs pH 8@3 h with CTPs pH 8@6.5 h) at relatively constant pH 8 condition and indicates clearly that the actual analyte gas composition is continuously changing over time. This, probably, may be due to the activity of the microorganisms in the analysis sample resulting in further production of biogas.

With transition to pH 5, intense gas evolution with foam formation was observed. This gas development was intense enough to escape through the backflow protection (water filled gas bubbler) (Fig. 3a) and was registered as highly increased sensor signals in time period 6.5–7.7 h (Fig. 6). It is represented in the corresponding CTPs of all MO-layers by a sharp characteristic peak between 1 and 3 min, for e.g., as observed for CTPs pH 5@7 h (Fig. 8).

Comparing the normalized CTPs (equalization of the conductance values at the peak temperature (Tmax)) measured at pH 8@3 h, pH 8@6.5 h and pH 5@7 h, for example, of SnO_2(FSP)/NASICON (Fig. 9a), reveals that the characteristic peaks observed in those three CTPs are all at the same position (at about 2.5 min) with respect to cycle time and sensor temperature (230 °C). This observation suggests that the surface reaction of the same gas component could be responsible for those sharp peaks. Besides, those characteristic features are in good resemblance to the CTP features observed in normalized CTP of SnO_2(FSP)/NASICON (Fig. 9a) at exposure to 2000 ppm CO with 50% relative humidity measured in the automated gas sensor test system [46]. Furthermore, the result (Fig. 7b) of an offline FTIR analysis experiment (Fig. 4c) of the gas collected during this intense gas development at pH 5 condition confirmed the presence of a small concentration of CO admixed with high amount of CO_2 and water vapor. However, the FTIR spectrum does not contain any absorption bands representing acetic or propionic acid vapours, but small characteristic features of these vapours are already observed in the CTPs (Fig. 9) at this pH-value. As a first conclusion, this means that at transition from pH 8 to pH 5 not only more and more undissociated VFA is formed (Fig. 2), but also this transition seems to trigger an alteration of the microbiological culture activity, which is observed as an intensive development of CO/CO_2 and, perhaps, other gas components like H_2, which are not IR-active. From the IR-spectrum (Fig. 7), it is concluded as well that the intense gas development is related to the formation of a high amount of gaseous CO_2 as pH is decreased from 8 to 5. The latter pH-value is clearly lower than the $pK_a = 6.5$ of the H_2CO_3/HCO_3^- - dissociation equilibrium (Eq. (2)) and, consequently, formation of CO_2 gas at pH-transition indicates a high concentration of bicarbonate dissolved at pH 8.

$$CO_2 + H_2O \leftrightarrow H_2CO_3 \xleftrightarrow{pK_a=6.5} H^+ + HCO_3^- \xleftrightarrow{pK_a=10.5} 2H^+ + CO_3^{2-} \quad (2)$$

This, however, is not in contradiction to the interpretation of the high sensor signals observed at this time period of foam forming (see discussion above), because the sensitivity of MOG is well known to be very low to CO_2 but quite high to CO.

The intense gas development ended abruptly without further change of pH at about 7.7 h. This is clearly indicated by a sharp drop of the response of all eight MO-layers (Fig. 6) and, correspondigly, by less characteristic peak shape at around 2–3 min in CTPs of all MO-layers (CTPs pH 5@8.5 h, Fig. 8). The response of most of the MO-layers is now, in fact, lower than the response recorded at pH 8 (6.5 h) except for SnO_2(SG)/Alumina and SnO_2(SG)/YSZ-layers. This is due to the fact that the CTP-response of the two latter layers is observed relatively low at

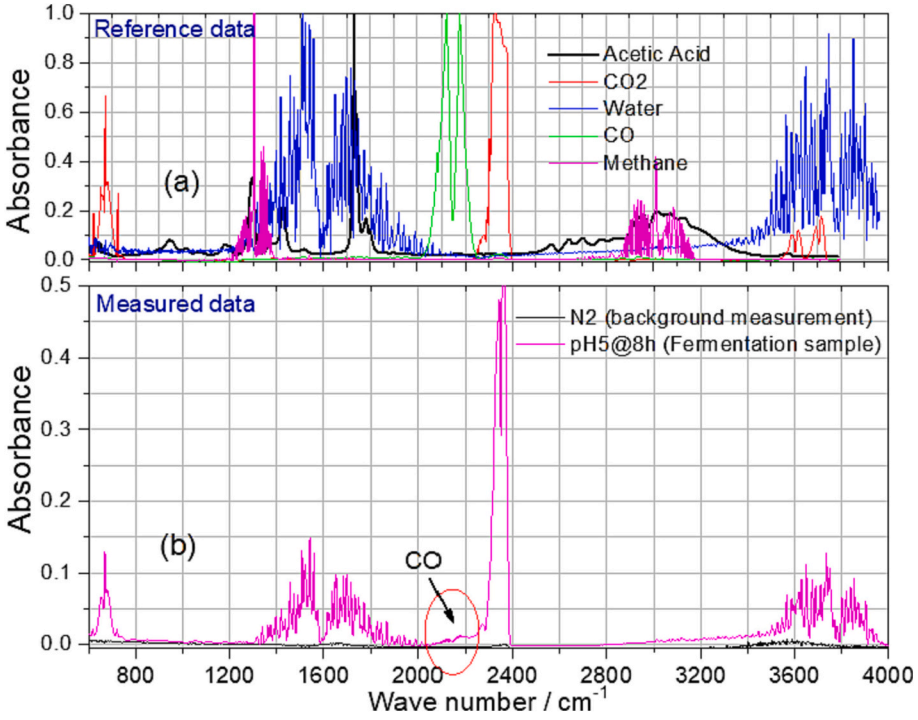

Fig. 7. FTIR analysis data. Sampled from intense gas evolution at pH 5 (a) Reference FTIR absorbance spectrum of acetic acid, CO_2, water, CO and CH_4 [45]. (b) Measured FTIR background spectrum with N_2 and FTIR spectrum of the gas extracted from the analysis sample.

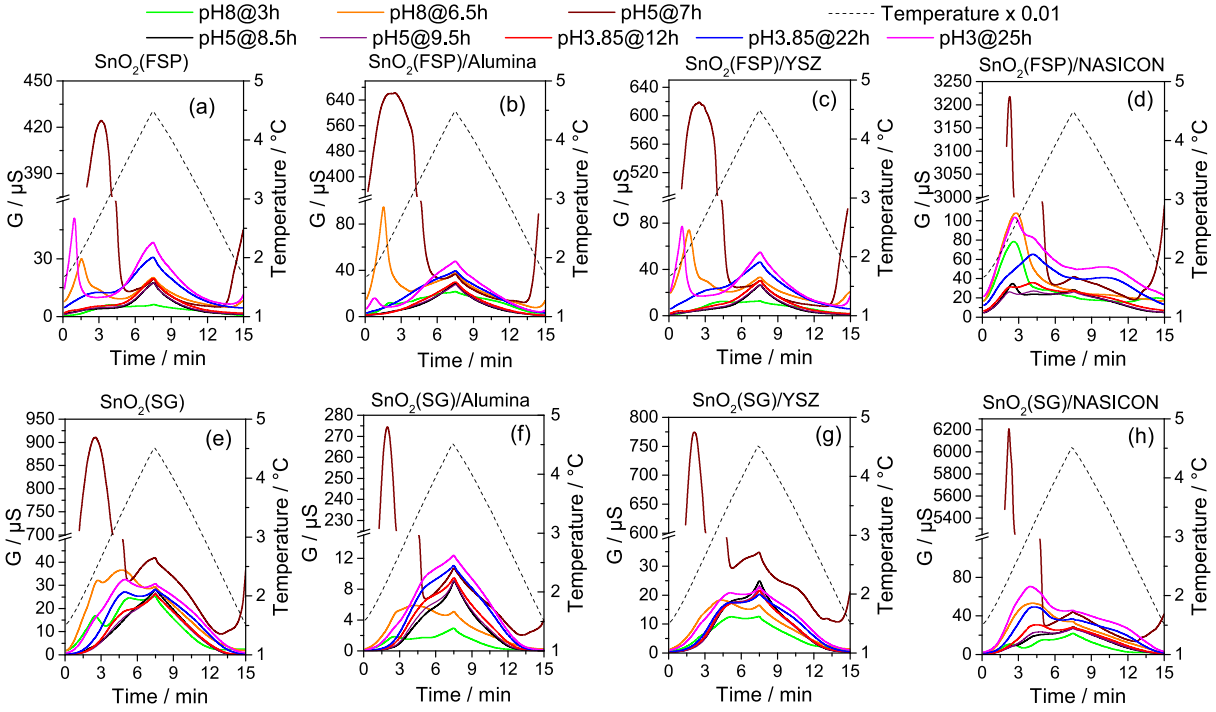

Fig. 8. CTPs of (a) SnO_2(FSP), (b) SnO_2(FSP)/Alumina, (c) SnO_2(FSP)/YSZ, (d) SnO_2(FSP)/NASICON, (e) SnO_2(SG), (f) SnO_2(SG)/Alumina, (g) SnO_2(SG)/YSZ, (h) SnO_2(SG)/NASICON as absolute conductance values at exposure to gases extracted by the CGP at different pH conditions of fermentation matrix.

pH 8 (6.5 h) in relation to the other layers. Further, CTPs shape at pH 5@8.5 h is clearly different compared to the CTPs shape at pH 8@6.5 h and, of course, also to the CTP shapes at pH 5@7 h (gas development, Fig. 8). These differences may be explained by the escape of gases from the analysis reactor during the intense gas development. The escaped gas may contain residual physically dissolved gases after N_2 purging, newly developed biogas components including other byproducts over time (1.75–6.5 h) and even some portion of undissociated VFAs, which equilibrated with the dissociated form as pH was shifted to 5. The intense evolution of CO_2 and correspondingly its high portion in the gas development may have an additional purging effect of the other (low concentrated) gas components.The latter assumption is supported by the

GC-analysis results (Fig. 6), which show a small, but significant decrease of the acetic and propionic acid concentrations after the foam formation/gas development event.

Post intense gas development (7.75–9.5 h), the resoponse of the MO-layers seems to be very stable (Fig. 6) at constant pH 5 condition. However, more detailed study of the CTP shapes (Fig. 8) revealed significant changes in the CTPs shape of SnO_2(FSP)/NASICON, SnO_2(SG)/NASICON and SnO_2(SG)/Alumina layer in the time interval over one hour from pH 5@8.5 h to pH 5@9.5 h. This is even better illustrated by the plot of the normalized CTPs of SnO_2(FSP)/NASICON and SnO_2(SG)/NASICON (Figs. 9a and c). The response of these layers seems to reflect the change in gas composition over time at best in good agreement with the former investigations [40]. Theoretically, substantial activity of methane-forming bacteria is not expected below pH 6 [25,47]. However, significant activity of acid-forming bacteria occurs above pH 5 [47]. Thus, development of biogas along with other byproducts cannot be excluded in this period of process.

After next step of pH-decrease to pH 3.85 (Fig. 6), namely to a value well below the pKa of the VFAs (4.87 and 4.76 for acetic and propionic acid, respectively), almost 90% of the VFAs are transformed to the undissociated state (Fig. 2) and, as expected, there is an increase of the response of all the MO-layers, which is better visualized as CTPs at pH 3.85@12 h (Fig. 8). These relatively small CTP-changes of all of the MO-layers (e.g., related to CTPs at pH 5@9.5 h) increased significantly over the time span of 10 h at constant pH 3.85 condition, and the CTPs became more and more characteristic (compare CTPs at pH 3.85@12 h with those CTPs at pH 3.85@22 h (Fig. 8)). Assuming that the small but significant increase of the CTP is not a consequence of a very slow signal response, this observation has to be interpreted as a slow increase of the VFA-concentrations (or other gas components) over time. At pH 3 which is now far below the pKa value of the VFAs, almost all the VFAs are in undissociated state (Fig. 2) and, as expected, the sensitivity of the measurement is highest for all the MO-layers resulting in highly specific CTP shape represented as pH 3@25 h (Fig. 8). But the CTPs of the different SnO_2/additive –layers are observed very different in intensity and shape specificity. The CTPs at pH 3@25 h of the FSP-layers (Figs. 8a – d) have an additional sharp peak at around 1 min in common, which is shifted to about 2.5 min in case of SnO_2(FSP)/NASICON –layer. The position of those peaks with respect to time and temperatue is clearly different to the peaks observed in the CTPs pH 8@6.5 and pH 5@7 h and they may represent the undissociated VFAs and/or other byproducts formed in state of pH 3. However, the CTP shape of SnO_2(FSP)/NASICON (Fig. 8d)at pH 3@25 h shows a very similar structure (double peak vs. peak and shoulder) as those observed at pH 3.85@12 h and even at pH 5@9.5 h. This again indicates that this composite-layer enables very sensitive VFA-analysis even at pH-states at which only a lower portion of the analyte can be measured in the undissociated state. The SnO_2(SG)/additive– layers show similar signal trends, but the CTP shapes are clearly less structurized and therefore less specific.

The exceptional sensing behavior of SnO_2(FSP)/NASICON and SnO_2(SG)/NASICON layers is even more impressively illustrated by comparing the normalized CTPs at pH 5@9.5 h, pH 3.85@22 h and pH 3@25 h (Figs. 9a andc). Comparing those normalized CTPs with those CTPs recorded at exposure with 100 ppm model acetic acid and propionic acid dissolved in DI water (Figs. 9b and d) reveals that the CTP features observed at different pH conditions of the fermentation samples are in good resemblace with the position of the peaks observed in measurements with the model VFAs. For instance, the peak observed at around 4 min of CTP pH 5@9.5 h, in case of SnO_2(FSP)/NASICON is specifically at the same position as observed for the propionic acid. Similarly, the relatively wide maxima observed in CTP pH 5@9.5 h at about 4.3 min for SnO_2(SG)/NASICON represents both, propionic and acidic acid peaks. As already stated above, it is quite impressive that SnO_2(FSP)/NASICON and SnO_2(SG)/NASICON-layers show such clear

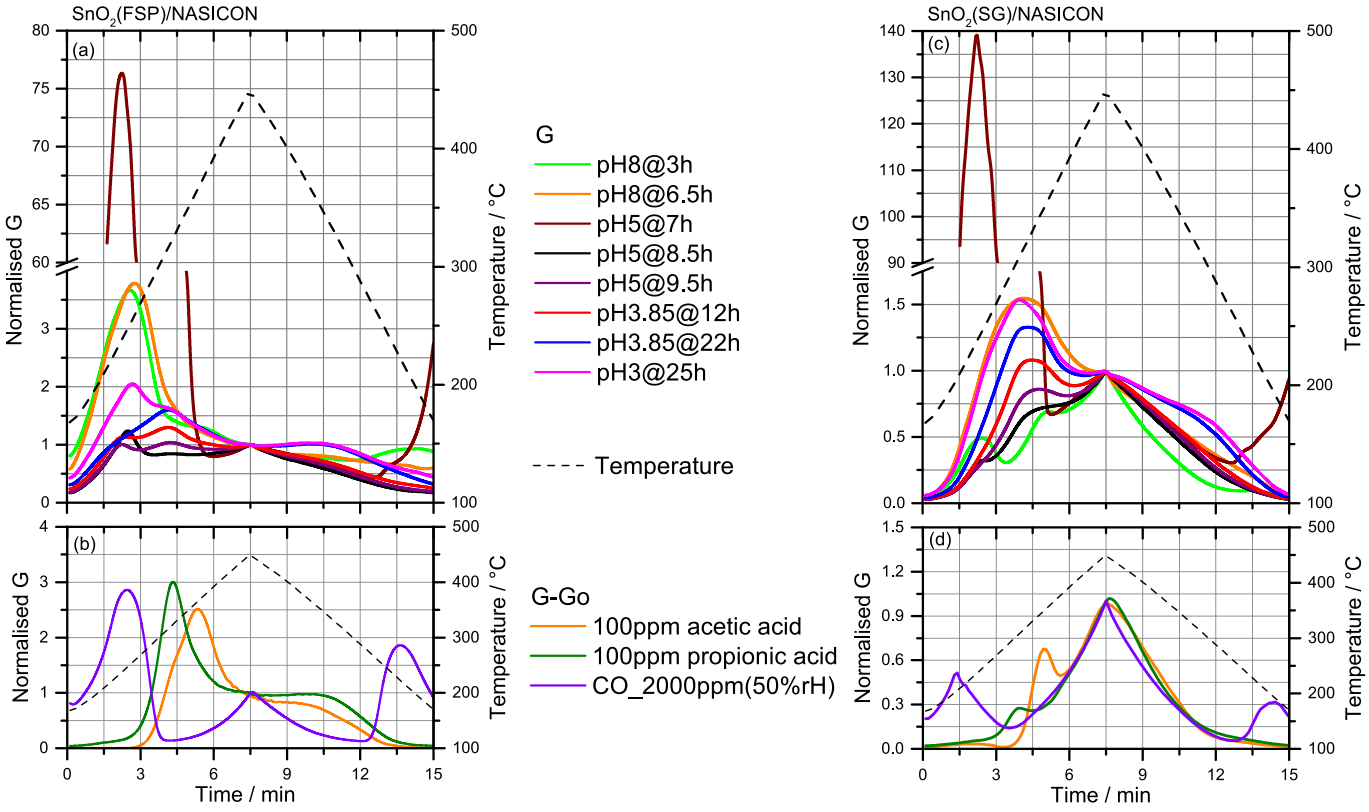

Fig. 9. Normalized CTPs of (a) SnO_2(FSP)/NASICON and (c) SnO_2(SG)/NASICON at different pH conditions of the fermentation sample. For comparison, the corresponding normalized CTPs, given as G-Go-values measured on model gases, are illustrated in (b) and (d). Go (used for CTP at 2000 ppm CO) is the reference CTP measured at synthetic air with 50%rH, whereas for the CTP-measurements of the dissolved acids Go was measured via CGP in DI water at pH 7.

variation in CTP shape and integral even for such small changes in un-dissociated VFA concentration at pH 5 (Fig. 9) with only around 36% and 43% (Fig. 2) of the dissolved acetate (115 ppm) and propionate (44 ppm) (Fig. 6), respectively, in un-dissociated state. This could be associated with the enhanced sensing behavior induced by NASICON [40,48]. The other SnO_2/additive layers do not show this correlation of the CTP shapes with the model acids so clearly (Fig. 10).

As an intermediate summary, the results clearly demonstrate the proof-of-concept that use of CGP after sample pre-conditioning (increase of pH for N_2-purging and then lowering of the pH value below pKa value of VFAs) enables the applicability of well selected SnO_2/additive gas sensitive layers for acetic/propionic acid analysis in biogas fermentation processes. Further, the MOGs could be used even for monitoring of the actual process condition as well. As shown by the results, the response of the MO-layers to any change in the gas composition is rather fast (at least two thermal cycle i.e., around 30 min). However, the time required for sample conditioning (N_2-purging) has to be considered as well. The detection limit of the MO-layers, for e.g., SnO_2(FSP)/NASICON and SnO_2(SG)/NASICON-layers is well below 100 ppm as shown by the results from the measurements at pH 5. In Sec. 4.2, the MO-layers response to higher changes in the VFA concentration will be discussed.

4.2. Sensor response and CTPs at varying VFA concentrations

In this Sec., the sensor responses to additional dosage of acetic and propionic acids into the fermentation sample are studied in relation to the CTPs measured at pH 3@25 h. By comparison of the corresponding CTP shapes, some disclosure about the correlations between those CTP shapes representing the "original fermentation matrix" and those achieved by increase of the acetic/propionic acid content in the fermentation liquid, is expected. An overview of the responses of the FSP and sol-gel prepared layers at differently adjusted acetic acid and propionic acid concentrations at pH 3 is given in Fig. 11. As a general trend, a clear stepwise increase of sensor response upon pH-change from 5 to 3 - as already discussed in Sec. 4.1 - and further addition of acetic acid (200 ppm, 500 ppm,1000 ppm and 2000 ppm) up to around 35th h was observed in all the MO-layers with different individual sensitivity. This stepwise response is more clearly illustrated for the FSP-layers related to the SG-layers, except for SnO_2(FSP)/Alumina, which shows no response to pH-change and to the first acetic acid dosage (1#). The corresponding CTPs measured at different acetic acid concentrations increased in steps by manual dosage and are visualized in Fig. 12. As a matter of fact, there is a monotonic increase of all the CTPs observed in relation to the CTPs measured at pH 3@25 h. In good agreement with the discussion in Sec. 4.1, this indicates that, indeed, the CTP-structure at pH 3@25 h is dominated by some acetic acid-content. The characteristic feature of FSP prepared layers is predominantly the sharp increase of the peak at around 1 min with increasing acetic acid concentration, which is shifted to about 3 min in case of the SnO_2(FSP)/NASICON –layer (Fig. 12d). In contrast, the SG-layers (Figs. 12e-h) are characterized by a double peak or shoulder/peak during heating phase (~3 min and 5 min) of the temperature cycle. This characteristic structure becomes more pronounced with increasing acetic acid concentration. Hypothetically, this may indicate roughly two different kinds of reaction sites, which may be a consequence of the much broader SnO_2 grain size distribution of the SG-prepared layers [40]. In case of SnO_2(SG)/NASICON, those two features are not well separated for lower acetic acid concentrations but could be clearly distinguished, for example, as double peak in CTP pH 3_2000ppm_ac.acid_35h (Fig. 12h).

The sensor response of FSP-layers and SnO_2(SG)/NASICON (Fig. 11) started to decrease abruptly without further change of pH or acetic acid concentration after the acetic acid concentration had reached 2000 ppm, with individual rate beyond ~35 h but with much lower rate beyond 37.5 h for the other SG-layers. The reason for this decrease of the sensor response is not clear up to now. It may indicate the change in gas composition over time by still running bio-fermentation processes. Such

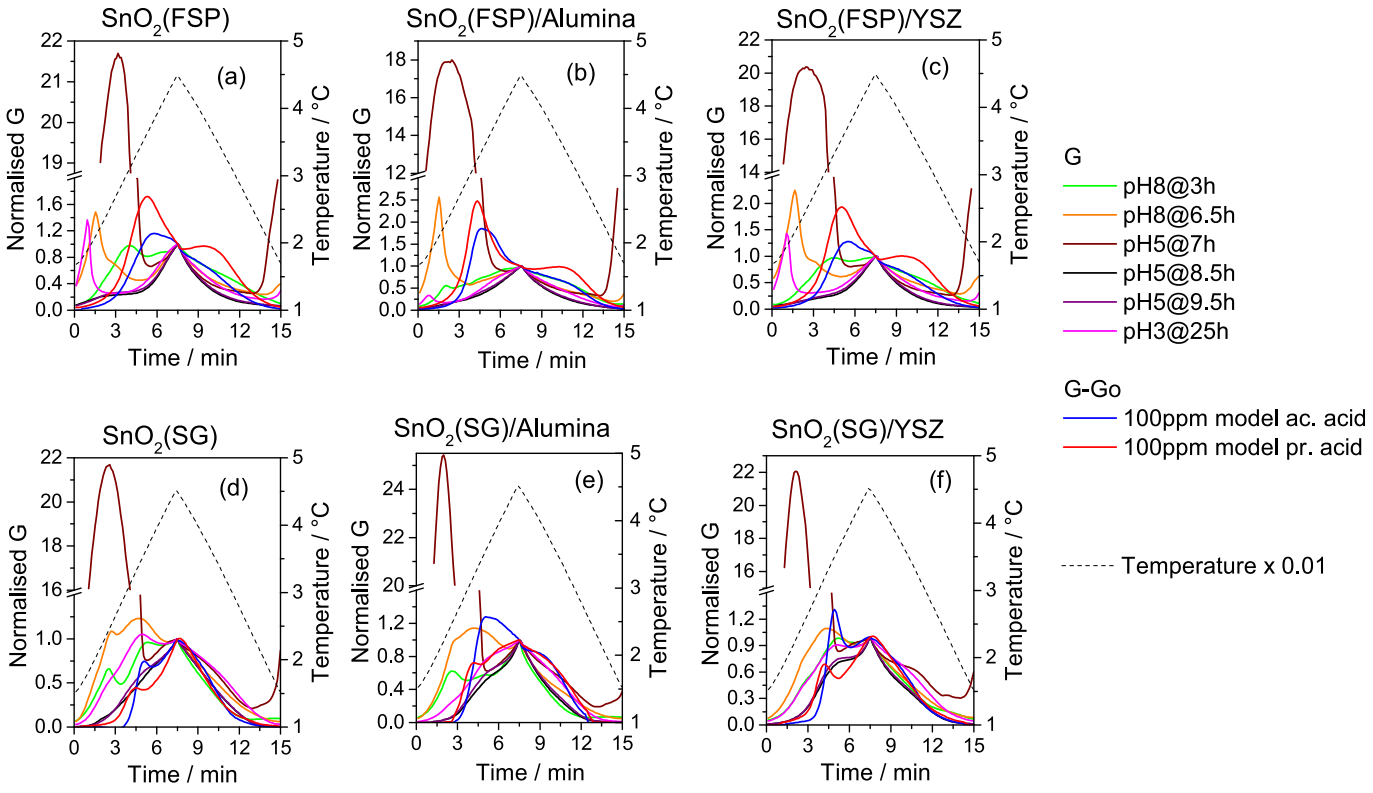

Fig. 10. Normalized CTPs of (a) SnO_2(FSP), (b) SnO_2(FSP)/Alumina, (c) SnO_2(FSP)/YSZ, (d) SnO_2(SG), (e) SnO_2(SG)/Alumina, (f) SnO_2(SG)/YSZ measured at different pH conditions (pH 8, pH 5 and pH 3). For comparison, the CTPs of 100 ppm acetic acid and 100 ppm propionic acid dissolved in DI water at pH 3 are visualized as normalized G-Go - values. Here, Go is the CTP measured in DI water at pH 7 [40].

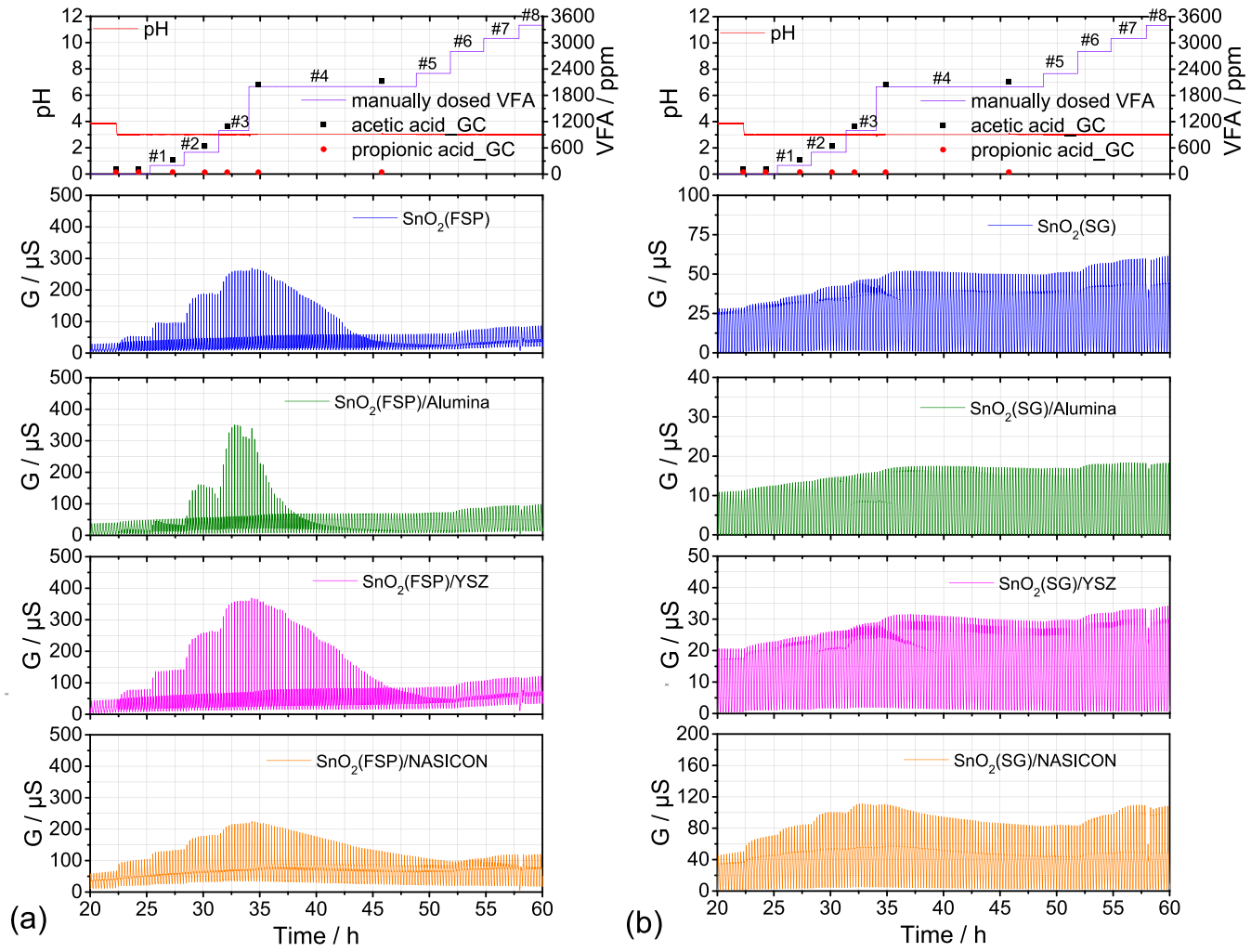

Fig. 11. Sensor response over time of different (a) SnO_2(FSP)/additive-layers and (b) SnO_2(SG)/additive-layers to different VFA concentrations (#1: 200 ppm acetic acid, #2: 500 ppm acetic acid, #3: 1000 ppm acetic acid, #4: 2000 ppm acetic acid, #5: 2300 ppm acetic acid, #6: 2300 ppm acid +500 ppm propionic acid, #7: 2300 ppm acid +800 ppm propionic acid, #8: 2600 ppm acid +800 ppm propionic acid) at pH 3 provided by additional dosage of the corresponding VFAs.

a change in the gas composition could be represented by the decrease of the most characteristic CTP-peak of the FSP-layers at ~1 min (Figs. 13a-c) and at ~2.5 min measured on the SnO_2(FSP)/NASICON–layer (Fig. 13d), respectively. Also the SG-layers show systematic decrease of the corresponding CTP-features, but with lower rate. Regarding the FSP-layers, this trend of CTP-change is opposite to that observed by dosage of acetic acid (Fig. 12), which could give rise to the assumption that decomposition of acetic acid is observed here (Fig. 13). However, this assumption is not so clearly confirmed by the CTP-changes of the SG-layers (Fig. 13).

Further addition of acetic acid at 48.8 h (Fig. 11) resulted in small but significant increase of the response of FSP layers (Fig. 11a) compared to SG-layers (Fig. 11b) which is better visualized in Fig. 14 (e.g., compare CTPs ph3_2000ppm_ac.acid@48.5 h and ph3_2300ppm_ac.acid@51.5 h). The response of SG-layers to acetic acid appears to be saturated which may be related to their lower signal range and lower sensitivity to acetic acid compared to the FSP layers [40]. However, the addition of 500 ppm and 800 ppm propionic acid at 51.5 h and 54.5 h resulted in a clear stepwise increase of the response of all the MO-layers (Fig. 11), which is even better illustrated in the CTPs (Fig. 14) by clear increase of the absolute conductance in the temperature range between 3 min (about 250 °C) and the peak temperature, i.e., clearly beyond the temperature where the main response to acetic acid was observed. This effect could be related to the higher sensitivity to propionic acid compared to acetic acid [40] and gives some hint for some ability to discriminate between both kinds of acids. Again, CTPs of SnO_2(FSP)/NASICON and SnO_2(SG)/NASICON, as well as SnO_2(FSP)/YSZ and SnO_2(SG)/YSZ, show excellent sensing behavior and specificity to acetic acid and propionic acid which will now be discussed a little bit closer. Further increase of acetic acid concentration (2000 ppm to 2300 ppm) shows decrease of the CTPs at the lower temperatures at 1 min respectively 1.5 min (Figs. 14c and d). Additional dosing of propionic acid results in a general increase of the CTPs, but major increase is observed at the higher temperatures between about 250 °C and 400 °C. Finally, further increase to 2600 ppm acetic acid leads to further decrease of the peak at 1.5 min measured on SnO_2(FSP)/NASICON (Fig. 14d), but to a general increase of conductance in the whole CTP-range in case of SnO_2(FSP)/YSZ (Fig. 14c).

These results show that there seems to be a clear correlation between the dosed VFA type and the CTP features. However, different kinds of correlations are observed at different layers, i.e. these may represent different surface processes dependent on the additive. In case of SnO_2(FSP)/NASICON, increase of acetic acid concentration seems to depress surface reactions represented by the CTP-peak at 1.5 min. This is not observed in the CTPs measured on SnO_2(SG)/NASICON (Fig. 14h), perhaps, due to less pronounced CTP-shape specificity.

A better overview of sensor response vs. VFA-dosage may be given by the dependency of the absolute sensor resoponse represented by the

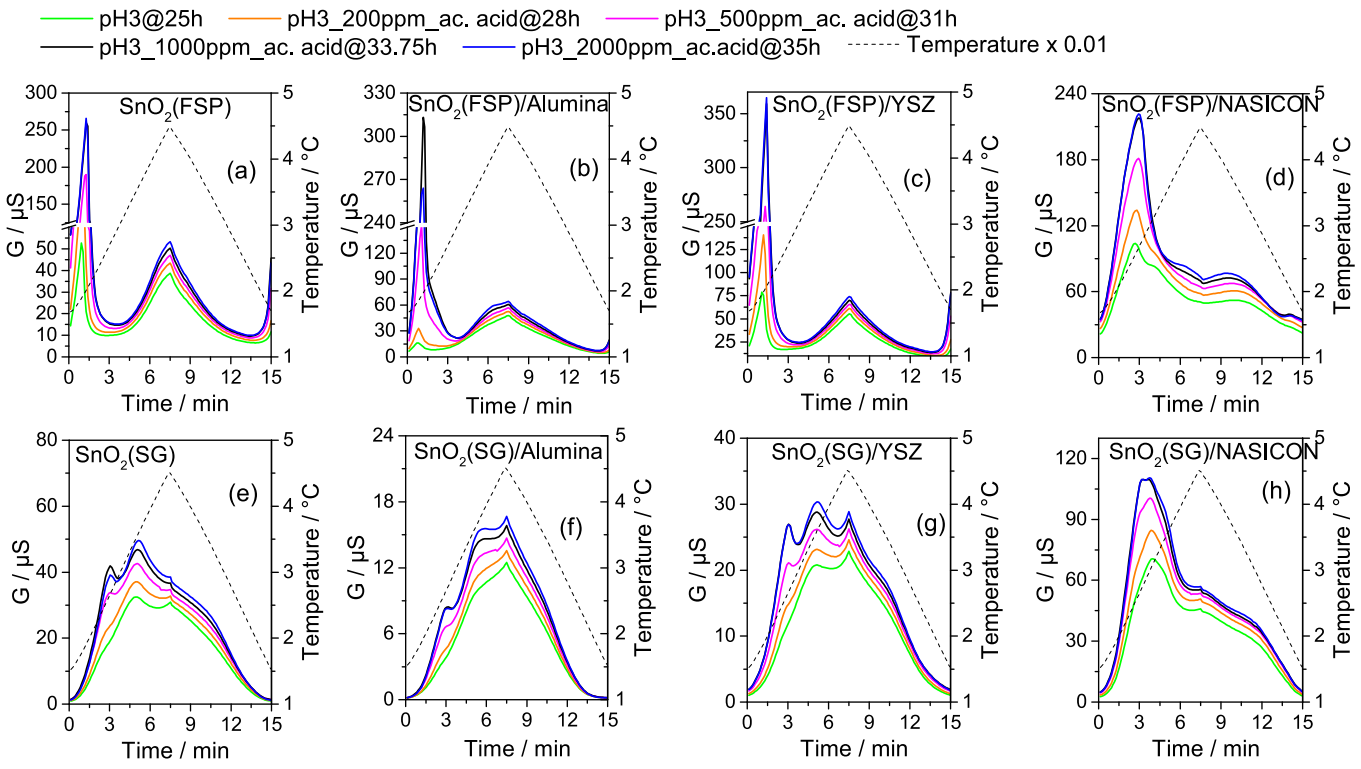

Fig. 12. CTPs measured as absolute conductance G of (a) SnO_2(FSP), (b) SnO_2(FSP)/Alumina, (c) SnO_2(FSP)/YSZ, (d) SnO_2(FSP)/NASICON, (e) SnO_2(SG), (f) SnO_2(SG)/Alumina, (g) SnO_2(SG)/YSZ, (h) SnO_2(SG)/NASICON at exposure to different acetic acid concentrations (200 ppm, 500 ppm, 1000 ppm, and 2000 ppm) in the fermentation matrix at pH 3.

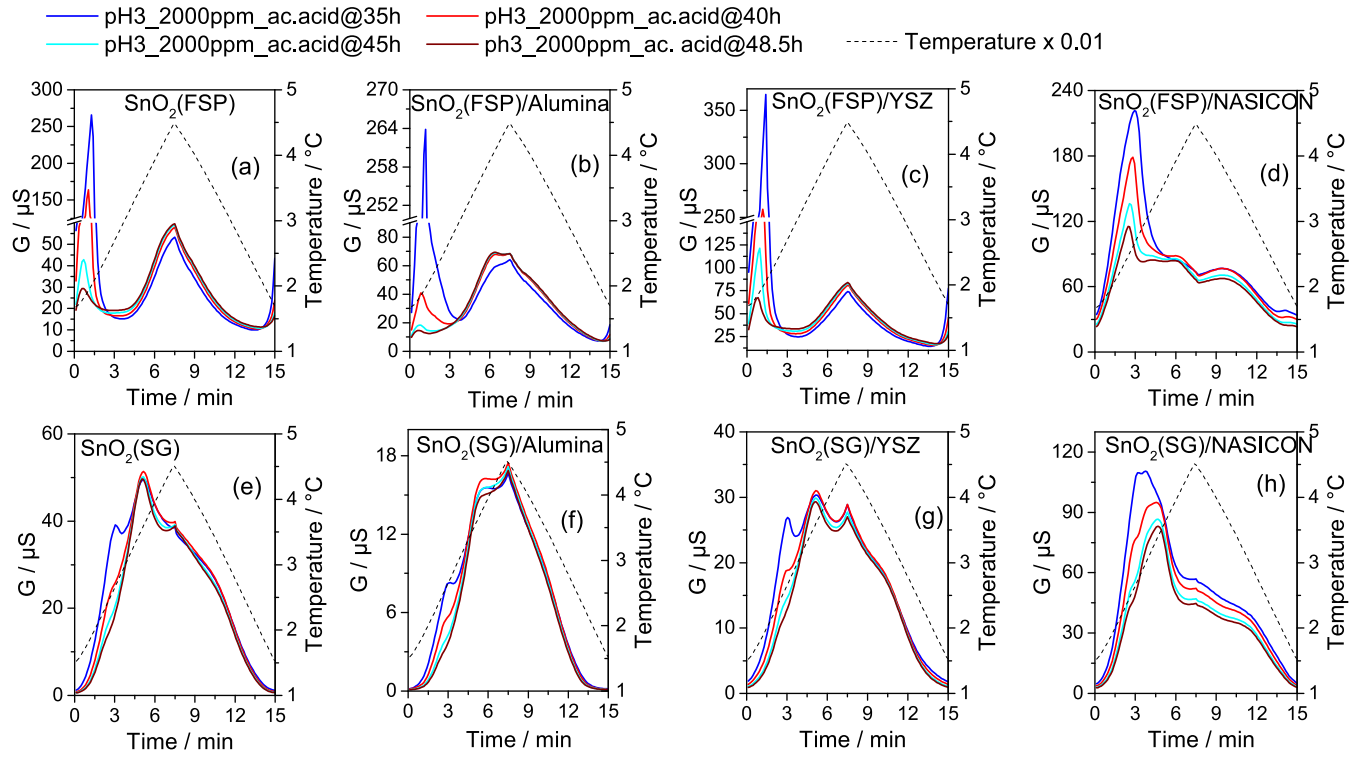

Fig. 13. CTPs measured as absolute conductance G of (a) SnO_2(FSP), (b) SnO_2(FSP)/Alumina, (c) SnO_2(FSP)/YSZ, (d) SnO_2(FSP)/NASICON, (e) SnO_2(SG), (f) SnO_2(SG)/Alumina, (g) SnO_2(SG)/YSZ, (h) SnO_2(SG)/NASICON at constant acetic acid concentration (2000 ppm) in the fermentation matrix at pH 3.

integral of the CTPs of different SnO_2/additive-layers as calculated according to Eq. (1) (both, acetic and propionic acid) at pH 3 condition (Fig. 15). In general, two different dependencies could be observed, one up to 1200 ppm, which represent pure acetic acid dosage, and the other at 2000 ppm VFA and beyond. The first dependency represents the situation between 20 h and 35 h (Fig. 11) of measurement whereas, the

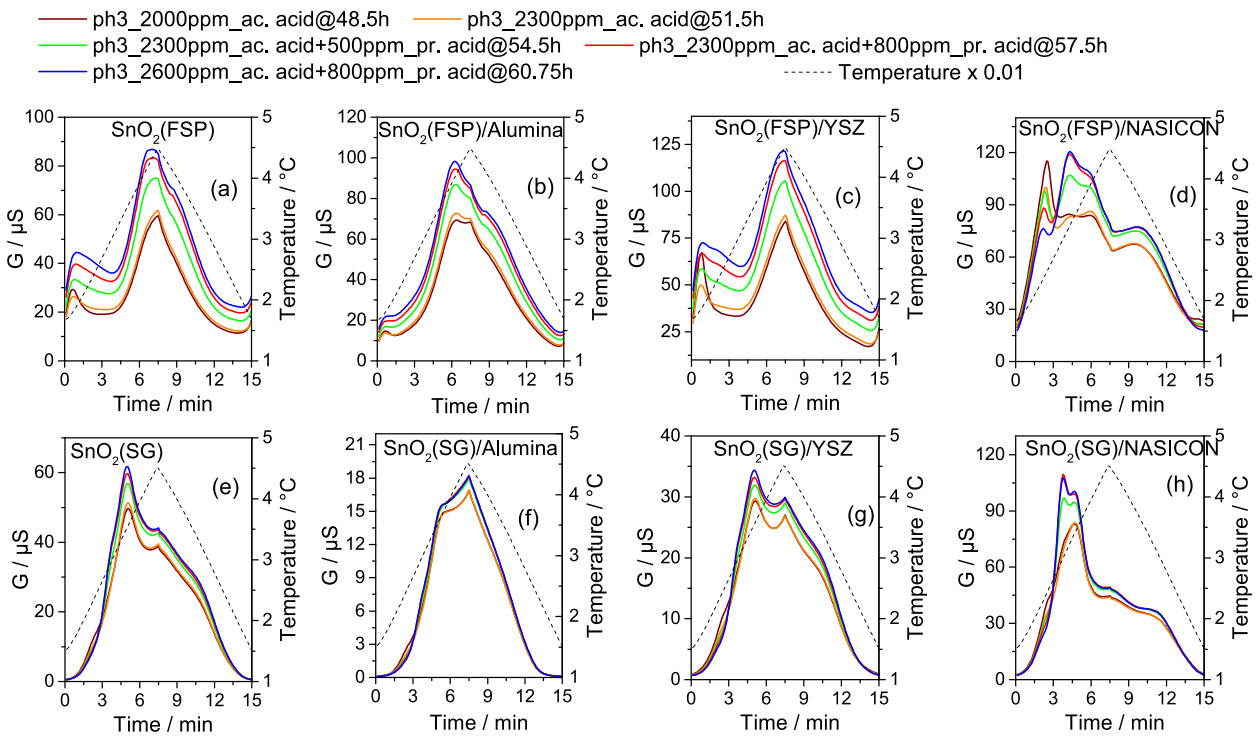

Fig. 14. CTPs measured as absolute conductance G of (a) SnO_2(FSP), (b) SnO_2(FSP)/Alumina, (c) SnO_2(FSP)/YSZ, (d) SnO_2(FSP)/NASICON, (e) SnO_2(SG), (f) SnO_2(SG)/Alumina, (g) SnO_2(SG)/YSZ, (h) SnO_2(SG)/NASICON after further increase of acetic acid and propionic acid concentrations in steps by manual dosage to the fermentation matrix at pH 3.

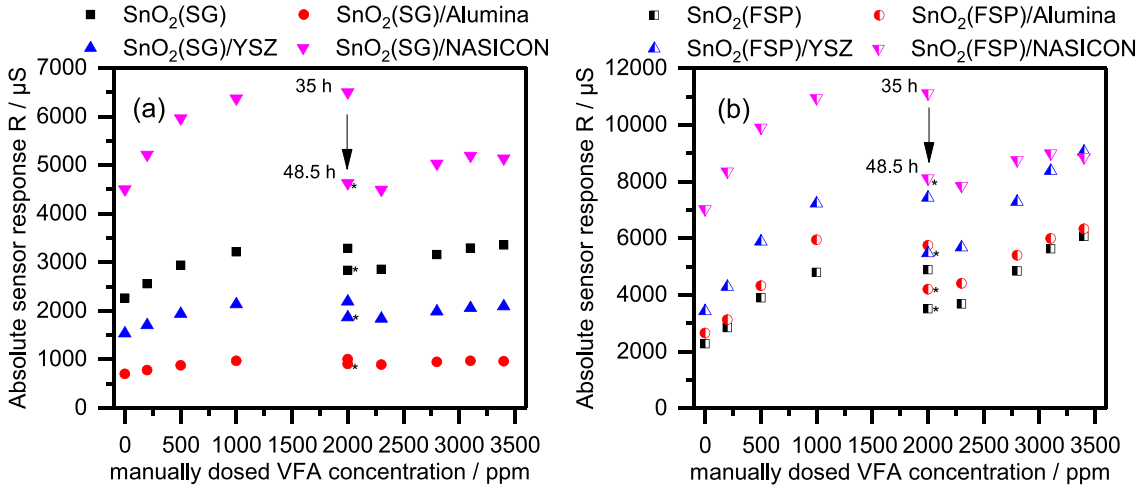

Fig. 15. Absolute sensor response (integral of CTP) of (a) different sol-gel prepared layers and, (b) FSP prepared layers vs. manually dosed VFAs concentration in fermentation sample at pH 3 condition as given in Figs. 12 and 14. Zero concentration value represents the total VFA concentration at pH 3 condition before dosage i. e., the sum of acetic and propionic acid concentrations as analyzed by GC analysis. The next concentration values represent the additional VFA concentration (acetic and propionic acid) manually dosed according to Fig. 4b. For 2000 ppm manually dosed VFA concentration two absolute sensor responses of each of the sensitive layers are presented. They represent the absolute sensor response at 35 h and 48.5 h (marked by *) and clearly indicate the decrease of the sensor response within this time span as observed in the CTPs in Fig. 13.

second dependency represents the CTP increase vs. acetic/propionic acid dosage (Fig. 14) after the considerable decrease of the CTPs within 13.5 h (35 h – 48.5 h) at constant acetic acid concentration (2000 ppm, Fig. 13).

Obviously, SnO_2(FSP)/additive-layers (Fig. 15b) show clearly higher absolute sensor response compared to SnO_2(SG)/additive-layers (Fig. 15a). However, among SnO_2(SG)/additive-layers (Fig. 15a) the CTP integrals of SnO_2(SG)/NASICON-layer are clearly the highest (Figs. 12 and 14). whereas among the FSP-layers (Fig. 15b) SnO_2(FSP)/NASICON layer shows highest absolute sensor response only to dosed acetic acid, but beyond 2000 ppm acetic acid, SnO_2(FSP)/YSZ shows highest sensitivity (CTP-integral change) vs. dosed propionic acid (Fig. 15b).

5. Conclusion and outlook

The intention of this work was to demonstrate that the quasi-online analysis of VFAs (acetic and propionic acid) in biogas fermentation

processes is possible by use of thermo-cyclically operated metal oxide gas sensor arrays complemented by a carrier gas probe. For demonstration and characterization of this advanced monitoring method, two sensor arrays each comprising a pure SnO_2 layer and three different SnO_2/additive composites (additives: alumina, YSZ, NASICON), were fabricated, but they differ by the SnO_2 preparation routes, namely Flame Spray Pyrolysis (FSP) and sol-gel (SG) preparation and, correspondingly, by the SnO_2-morphology.

The challenge was to analyze the development of the VFAs during the fermentation process in presence of high concentrations of biogas (CO, H_2, CH_4, etc.). Faced to the well-known cross sensitivity of MOG sensors to those biogas components, a pre-treatment process had to be introduced to get rid of the biogas without loss of the VFAs. This was possible by purging with N_2 for 45 min at pH 8. After decrease of the pH to three in several steps by dosage of phosphorous acid, the gas sensing behavior of the pure SnO_2 and SnO_2/additive-layers could be investigated by analysis of the Conductance over Time Profiles (CTPs) measured. These measurements at different pH conditions (pH 8, pH 5, pH 3.85 and pH 3) allowed variation of the fraction of undissociatively dissolved VFAs in the fermentation sample, their concentration in the carrier gas and, consequently, their influence on the CTPs. This means, by analysis of the corresponding CTP shapes the CTP-features representing the VFAs could be identified. All these experiments were referenced by GC-analysis. Obviously, CTPs measurements at pH 3, which is well below the pKa value of the VFAs (about pH 4.8), means that all the VFAs are in undissociated state and yield most pronounced CTP-features representing the VFAs. According to the authors knowledge, this kind of quasi online monitoring of VFAs by use of MOGs as introduced in this work, is reported for the first time. For better verification of the CTP-features representing the VFAs, CTPs at different VFA-concentrations experimentally simulated by manual dosage of acetic acid and propionic acid to the fermentation sample at pH 3 were measured as well and their rather similar shape characteristics to the CTPs measured for the original fermentation liquid at pH 3 was confirmed.

An essential part of this work are the experimental facts that the additives and the SnO_2/additive-layer morphology take profound influence on the CTPs. The FSP-prepared layers show clearly better sensitivity compared to SG-prepared layers and provide CTP specificity of higher quality. This is related to the particular morphology consisting of nano-scaled fine SnO_2-grains with extremely high surface to volume ratio of the grains, very narrow grain size distribution, very high porosity and, probably, higher surface state energy.

Some preliminary investigation results showed that the gas development triggered by lowering of the pH value of the fementation matrix from pH 8 to pH 5 and the continuous change of the analyte gas composition over time take clear influence on the CTPs of the SnO_2/additive-layers. This means, it could be clearly demonstrated that these changes of the CTP shape reflect changes of the actual biochemical situations, although the underlying biochemical reaction processes are not yet known in detail. In particular, the CTPs of SnO_2(FSP)/NASICON and SnO_2(SG)/NASICON were found to show very high sensitivity and strikingly enhanced specificity to acetic and propionic acid and are remarkably well reproducible. These outstanding sensing characteristics were related to special e^-/Na^+ – interactions across the SnO_2/NASICON interface, as already reported in earlier studies.

Finally, these preliminary studies clearly show that thermo-cyclically operated tin oxide gas sensors could be very interesting candidates for early in-situ monitoring of developing VFA in biogas fermentation processes if appropriate additives well adapted to the analysis problem, for example, highly sensitive SnO_2(FSP)/NASICON-composites, allow the extraction of representative CTP-features of the target gas component. However, further studies will be necessary in future (i) to correlate those CTP-features with the underlying biochemical processes and (ii) to gain quantitative VFA-concentration data by numerical analysis of the CTPs after calibration of the sensor elements and (iii) to develop a numerical CTP-analysis procedure, as introduced in Sec. 1, to quantify the VFA-concentrations. However, also machine learning methods may be interesting and even more economic in this context, if they are enabled to learn analysis of the VFA representing CTP-features from repeated sampling of the CTPs at changing fermentation environments. In this context, even further enhancement of the analysis quality provided by the SnO_2(FSP)/additive-composite is expected, if the homogenity of the SnO_2(FSP)/additive-composites, in particular the SnO_2(FSP)/NASICON-composite, could be considerably enhanced, i.e. the additive powder could be prepared even finer (e.g., by extended ball-milling or by modification of the preparation route) with grain size comparable to those of SnO_2 powder prepared by FSP technique. This would probably further enhance the sensitivity amplification effects, as already assumed in a hypothetical model for SnO_2/NASICON-composites in the past.

CRediT authorship contribution statement

Binayak Ojha: Methodology, Investigation, Formal analysis, Software, Visualization, Data curation, Writing – original draft, Writing – review & editing. **Andreas Wilke:** Funding acquisition, Investigation, Formal analysis. **Regina Brämer:** Formal analysis. **Matthias Franzreb:** Writing – review & editing. **Heinz Kohler:** Conceptualization, Methodology, Writing – original draft, Writing – review & editing, Supervision, Project administration, Funding acquisition.

Declaration of Competing Interest

The authors report no declarations of interest.

Data availability

Data will be made available on request.

Acknowledgements

We are deeply grateful to Prof. Dr. Andreas Güntner, Dept. of Mechanical and Process Engineering, ETH Zürich (CH). for providing the FSP-prepared SnO_2 powder. This work is part of the EBIPREP collaboration project (www.ebiprep.eu) financed by the EU International Programme INTERREG V Oberrhein 2017-2020.

References

[1] A. Schievano, G. D'Imporzano, F. Adani, Substituting energy crops with organic wastes and agro-industrial residues for biogas production, J. Environ. Manag. 90 (2009) 2537–2541.
[2] D. Artanti, R.R. Saputro, B. Budiyono, Biogas production from cow manure, Int. J. Renewab. Energy Develop. 1 (2012) 61–64.
[3] A.M. Pérez-Chávez, L. Mayer, E. Albertó, Mushroom cultivation and biogas production: a sustainable reuse of organic resources, Energy Sustain. Dev. 50 (2019) 50–60.
[4] B. Dhungana, S.P. Lohani, M. Marsolek, Anaerobic co-digestion of food waste with livestock manure at ambient temperature: a biogas based circular economy and sustainable development goals, Sustainability 14 (2022) 3307.
[5] L. Deressa, S. Libsu, R.B. Chavan, D. Manaye, A. Dabassa, Production of biogas from fruit and vegetable wastes mixed with different wastes, eer 3 (2015) 65–71.
[6] N.H. Garcia, A. Mattioli, A. Gil, N. Frison, F. Battista, D. Bolzonella, Evaluation of the methane potential of different agricultural and food processing substrates for improved biogas production in rural areas, Renew. Sust. Energ. Rev. 112 (2019) 1–10.
[7] A.O. Wagner, C. Reitschuler, P. Illmer, Effect of different acetate:propionate ratios on the methanogenic community during thermophilic anaerobic digestion in batch experiments, Biochem. Eng. J. 90 (2014) 154–161.
[8] L. Martín-González, X. Font, T. Vicent, Alkalinity ratios to identify process imbalances in anaerobic digesters treating source-sorted organic fraction of municipal wastes, Biochem. Eng. J. 76 (2013) 1–5.
[9] A. Costa, F. Maria Tangorra, M. Zaninelli, R. Oberti, A. Guidobono Cavalchini, G. Savoini, M. Lazzari, Evaluating an e-nose ability to detect biogas plant efficiency: a case study, Ital. J. Anim. Sci. 15 (2016) 116–123.
[10] K. Boe, D.J. Batstone, I. Angelidaki, An innovative online VFA monitoring system for the anerobic process, based on headspace gas chromatography, Biotechnol. Bioeng. 96 (2007) 712–721.
[11] L. Björnsson, M. Murto, B. Mattiasson, Evaluation of parameters for monitoring an anaerobic co-digestion process, Appl. Microbiol. Biotechnol. 54 (2000) 844–849.

[12] B.K. Ahring, M. Sandberg, I. Angelidaki, Volatile fatty acids as indicators of process imbalance in anaerobic digestors, Appl. Microbiol. Biotechnol. 43 (1995) 559–565.
[13] D. Platošová, J. Rusín, J. Platoš, K. Smutná, R. Buryjan, Case study of anaerobic digestion process stability detected by dissolved hydrogen concentration, Processes 9 (2021) 106.
[14] R.F. Hickey, M.S. Switzenbaum, The response and utility of hydrogen and carbon monoxide as process indicators of anaerobic digesters subject to organic and hydraulic overloads, Res. J. Water Pollut. Control Federat. 63 (1991) 129–140.
[15] P.F. Pind, I. Angelidaki, B.K. Ahring, A new VFA sensor technique for anaerobic reactor systems, Biotechnol. Bioeng. 82 (2003) 54–61.
[16] H.M. Falk, P. Reichling, C. Andersen, R. Benz, Online monitoring of concentration and dynamics of volatile fatty acids in anaerobic digestion processes with mid-infrared spectroscopy, Bioprocess Biosyst. Eng. 38 (2015) 237–249.
[17] J. Kretzschmar, L.F.M. Rosa, J. Zosel, M. Mertig, J. Liebetrau, F. Harnisch, A microbial biosensor platform for inline quantification of acetate in anaerobic digestion: potential and challenges, Chem. Eng. Technol. 39 (2016) 637–642.
[18] D.-J. Lee, S.-Y. Lee, J.-S. Bae, J.-G. Kang, K.-H. Kim, S.-S. Rhee, J.-H. Park, J.-S. Cho, J. Chung, D.-C. Seo, Effect of volatile fatty acid concentration on anaerobic degradation rate from field anaerobic digestion facilities treating food waste leachate in South Korea, J. Chemother. 2015 (2015) 1–9.
[19] H. Sun, J. Guo, S. Wu, F. Liu, R. Dong, Development and validation of a simplified titration method for monitoring volatile fatty acids in anaerobic digestion, Waste Managem. (New York, N.Y.) 67 (2017) 43–50.
[20] E. Palacio-Barco, F. Robert-Peillard, J.-L. Boudenne, B. Coulomb, On-line analysis of volatile fatty acids in anaerobic treatment processes, Anal. Chim. Acta 668 (2010) 74–79.
[21] S. Theuerl, J. Klang, A. Prochnow, Process disturbances in agricultural biogas production—causes, mechanisms and effects on the biogas microbiome: a review, Energies 12 (2019) 365.
[22] H.B. Nielsen, H. Uellendahl, B.K. Ahring, Regulation and optimization of the biogas process: propionate as a key parameter, Biomass Bioenergy 31 (2007) 820–830.
[23] G. Li, F. Xu, T. Yang, X. Wang, T. Lyu, Z. Huang, Microbial behavior and influencing factors in the anaerobic digestion of distiller: a comprehensive review, Fermentation 9 (2023) 199.
[24] D.T. Hill, S.A. Cobb, J.P. Bolte, Using volatile fatty acid relationships to predict anaerobic digester failure, Trans. ASAE 30 (1987) 496–501.
[25] K. Boe, Online Monitoring and Control of the Biogas Process, Dissertation, 2006.
[26] K. Maurus, N. Kremmeter, S. Ahmed, M. Kazda, High-resolution monitoring of VFA dynamics reveals process failure and exponential decrease of biogas production, Biomass Conv. Bioref. 13 (2023) 10653–10663.
[27] A. Patel, A. Mahboubi, I.S. Horváth, M.J. Taherzadeh, U. Rova, P. Christakopoulos, L. Matsakas, Volatile fatty acids (VFAs) generated by anaerobic digestion serve as feedstock for freshwater and marine oleaginous microorganisms to produce biodiesel and added-value compounds, Front. Microbiol. 12 (2021) 614612.
[28] A.T. Giduthuri, B.K. Ahring, Current status and prospects of valorizing organic waste via arrested anaerobic digestion: production and separation of volatile fatty acids, Fermentation 9 (2023) 13.
[29] K. Szacherska, P. Oleskowicz-Popiel, S. Ciesielski, J. Mozejko-Ciesielska, Volatile fatty acids as carbon sources for polyhydroxyalkanoates production, Polymers 13 (2021).
[30] B.J.J. Purser, S.-M. Thai, T. Fritz, S.R. Esteves, R.M. Dinsdale, A.J. Guwy, An improved titration model reducing over estimation of total volatile fatty acids in anaerobic digestion of energy crop, animal slurry and food waste, Water Res. 61 (2014) 162–170.
[31] M.J. Playne, Determination of ethanol, volatile fatty acids, lactic and succinic acids in fermentation liquids by gas chromatography, J. Sci. Food Agric. 36 (1985) 638–644.
[32] T. Becker, R. Kittsteiner-Eberle, T. Luck, H.-L. Schmidt, On-line determination of acetic acid in a continuous production of Acetobacter aceticus, J. Biotechnol. 31 (1993) 267–275.
[33] N. Tippkötter, A. Deterding, R. Ulber, Determination of acetic acid in fermentation broth by gas-diffusion technique, Eng. Life Sci. 8 (2008) 62–67.
[34] C. Wolf, D. Gaida, A. Stuhlsatz, S. McLoone, M. Bongards, Organic Acid Prediction in Biogas Plants Using UV/vis Spectroscopic Online-Measurements, Springer, Berlin, Heidelberg, 2010, pp. 200–206.
[35] H.F. Jacobi, C.R. Moschner, E. Hartung, Use of near infrared spectroscopy in monitoring of volatile fatty acids in anaerobic digestion, Water Sci. Technol. J. Int. Assoc. Water Pollut. Res. 60 (2009) 339–346.
[36] Andrea Stockl, Daniel Loeffler, Hans Oechsner, Thomas Jungbluth, Klaus Fischer, Martin Kranert, Near-infrared-reflection spectroscopy as measuring method to determine the state of the process for automatic control of anaerobic digestion, International Journal of Agricultural and Biological Engineering 6 (2013) 63–72.
[37] X. Jin, X. Li, N. Zhao, I. Angelidaki, Y. Zhang, Bio-electrolytic sensor for rapid monitoring of volatile fatty acids in anaerobic digestion process, Water Res. 111 (2017) 74–80.
[38] D.L. Röhlen, J. Pilas, M. Dahmen, M. Keusgen, T. Selmer, M.J. Schöning, Toward a hybrid biosensor system for analysis of organic and volatile fatty acids in fermentation processes, Front. Chem. 6 (2018) 284.
[39] K. Frank, V. Magapu, V. Schindler, H. Kohler, H.B. Keller, R. Seifert, Chemical analysis with tin oxide gas sensors: choice of additives, method of operation and analysis of numerical signal, Sens. Lett. 6 (2008) 908–911.
[40] B. Ojha, M. Aleksandrova, M. Schwotzer, M. Franzreb, H. Kohler, Thermo-cyclically operated metal oxide gas sensor arrays for analysis of dissolved volatile organic compounds in fermentation processes: part I – morphology aspects of the sensing behavior, Sens. Bio-Sens. Res. 40 (2023) 100558.
[41] R. Seifert, H.B. Keller, K. Frank, H. Kohler, ProSens—an efficient mathematical procedure for calibration and evaluation of tin oxide gas sensor data, Sens. Lett. 9 (2011) 7–10.
[42] N. Illyaskutty, J. Knoblauch, M. Schwotzer, H. Kohler, Thermally modulated multi sensor arrays of SnO2/additive/electrode combinations for enhanced gas identification, Sensors Actuators B Chem. 217 (2015) 2–12.
[43] S. Ciesielski, E.O. Adu, J. Mozejko-Ciesielska, T. Pokoj, A. Wilke, Wood Juice Valorization through Production of Poly(3-hydroxybutyrate- co −3-hydroxyvalerate) Using Bacillus sp. G8_19, ACS Sustain. Chem. Eng. 9 (2021) 16870–16873.
[44] Stefan Turad, Andreas Wilke, Joachim Jochum, Increasing efficiency and profitability of biogas plants by reducing the residence time and using a waste material-wood juice, in: Janusz Golaszewski, Irena Wojnowska-Baryla, Ewelina Olba-Ziety (Eds.), The 6th International Environmental Best Practices Conference "Sustainability schemes for bio-based products in the framework of the circular bioeconomy", Wydawnictwo Uniwersytetu Warminsko-Mazurskiego w Olsztynie, 2019, p. 181.
[45] P. Linstrom, NIST Chemistry WebBook, NIST Standard Reference Database 69, National Institute of Standards and Technology, 1997.
[46] A. Jerger, H. Kohler, F. Becker, H.B. Keller, R. Seifert, New applications of tin oxide gas sensors: II. Intelligent sensor systemfor reliable monitoring of ammonia leakages, Sensors Actuators B Chem. 81 (2002) 301–307.
[47] Alkalinity and pH, in: M.H. Gerardi (Ed.), The Microbiology of Anaerobic Digesters, John Wiley & Sons, Inc, Hoboken, NJ, USA, 2003, pp. 99–103.
[48] A. Hetznecker, H. Kohler, U. Guth, Enhanced studies on the mechanism of gas selectivity and electronic interactions of SnO2/Na+−ionic conductors, Sensors Actuators B Chem. 120 (2007) 378–385.